# The El Nino Southern Oscillation
# ENSO

A global coupled atmosphere-ocean phenomenon
seated in the tropics, with variability at 3-7 years

Ocean:  warm/cold waters off the coast of Peru (El Nino/La Nina)

Atmosphere:  pressure and wind variations (Southern Oscillation)

https://www.cpc.ncep.noaa.gov/ (click on ENSO in left menu)

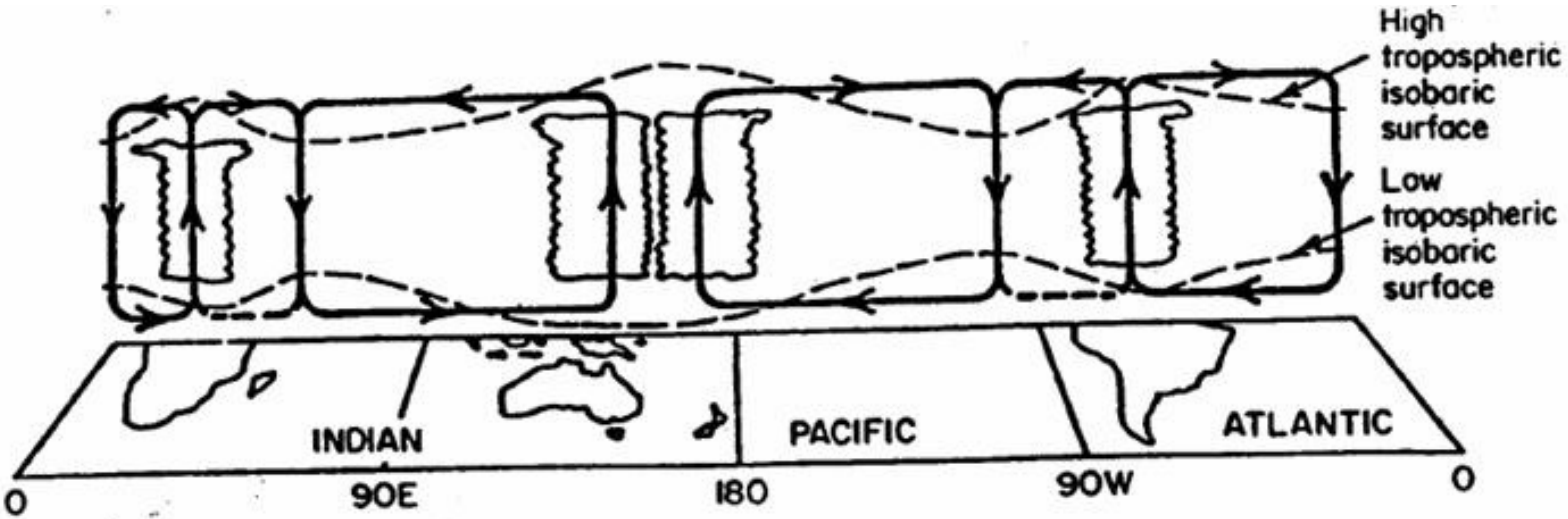


Figure 3.8 Schematic view of the east-west Walker circulation along the equator indicating low-level convergence in regions of convection where mean upward motion occurs. [From Webster (1983).]

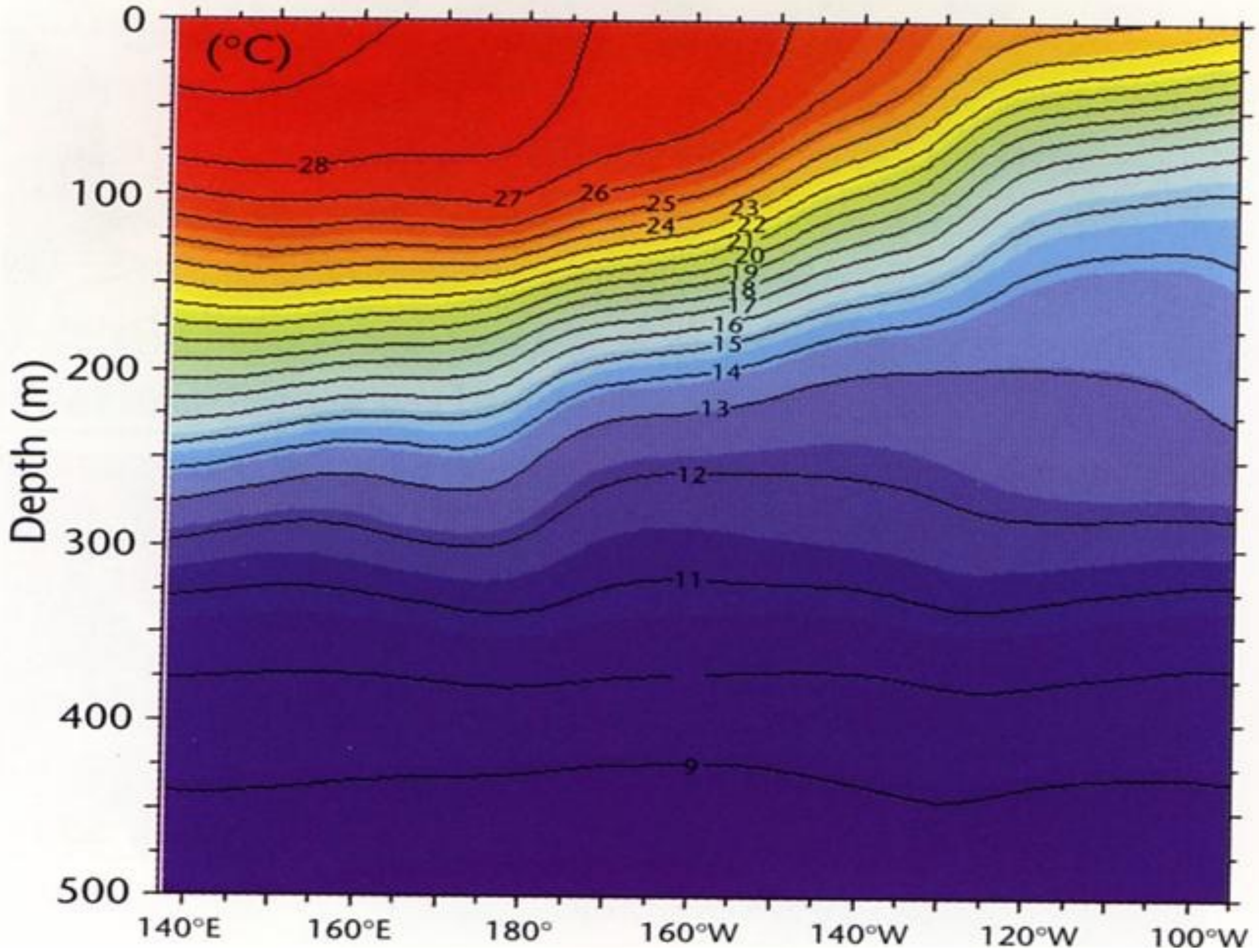


Figure 3.13. Vertical section along the equatorial Pacific showing the sloping thermocline, contour interval 1 K [www.cpc.noaa.gov].

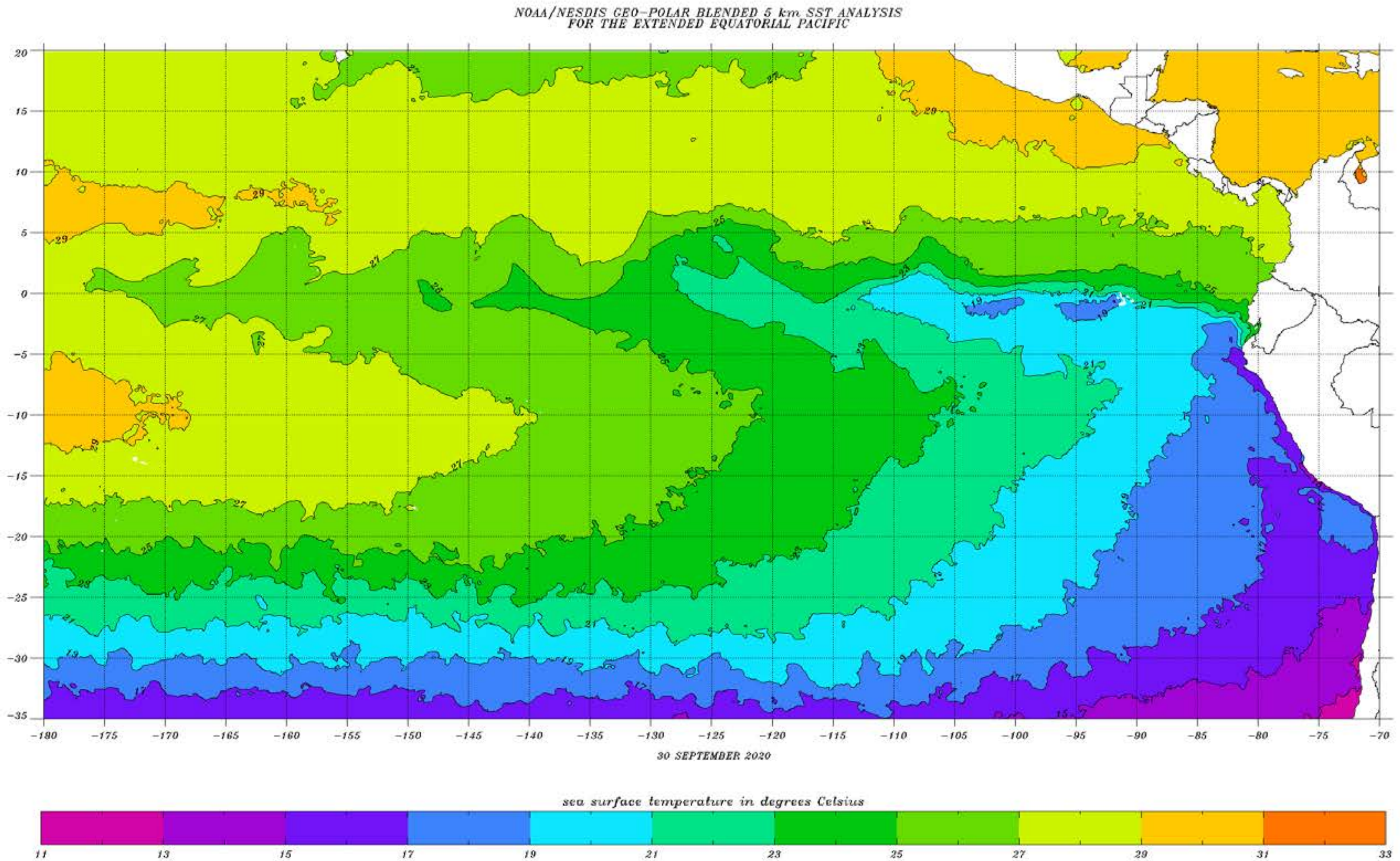


Northward winds along the coast drive offshore flow and upwelling.

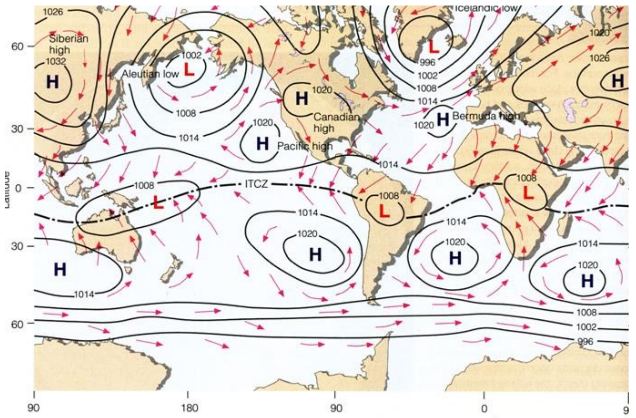


January

## La Niña

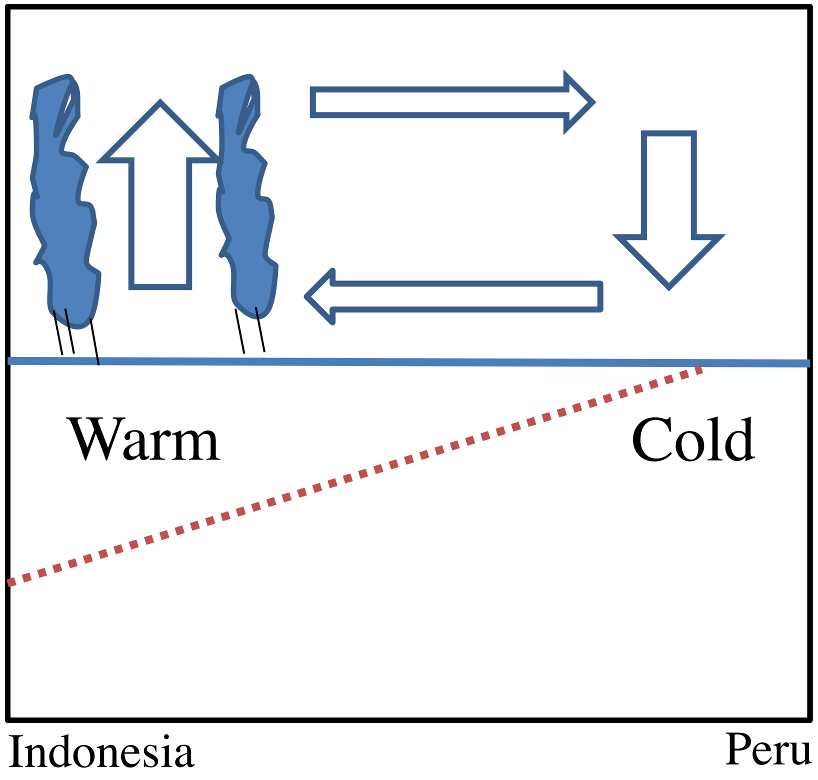


Strong Walker Circulation
Steeply-sloping thermocline
Cold SST/dry near Peru
Wet near Indonesia
Large Tahiti-Darwin SLP diff.

## El Niño

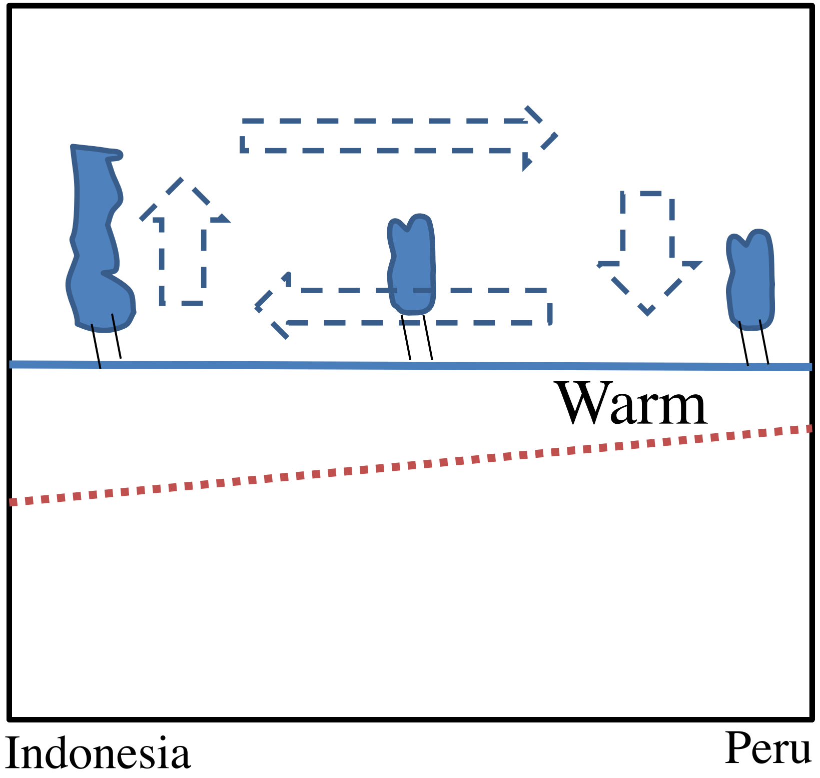


Weak Walker Circulation
Flat thermocline
Warm SST/wet near Peru
Dry near Indonesia
Small Tahiti-Darwin SLP diff.

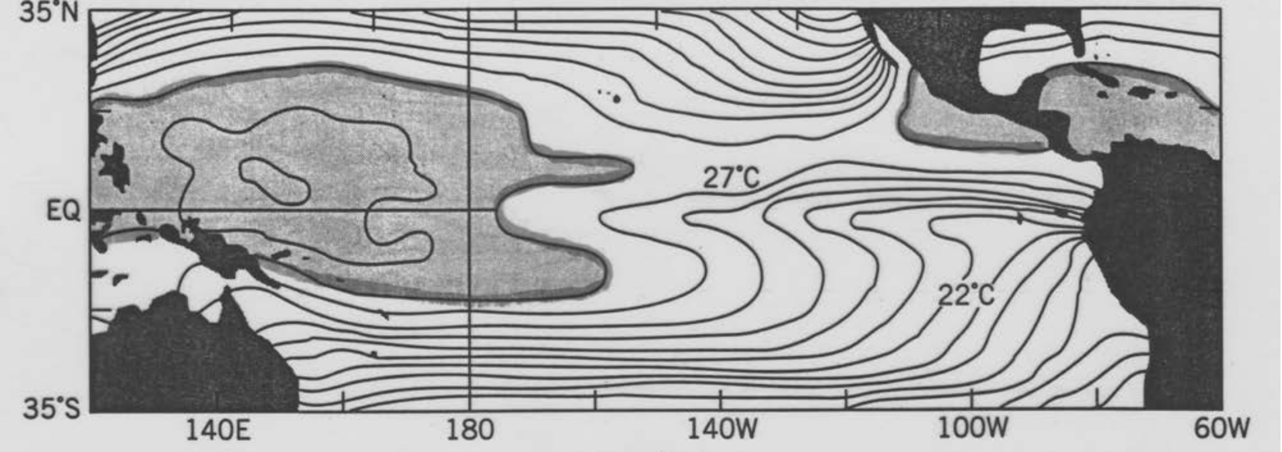


Time Mean SSTs
(for October)

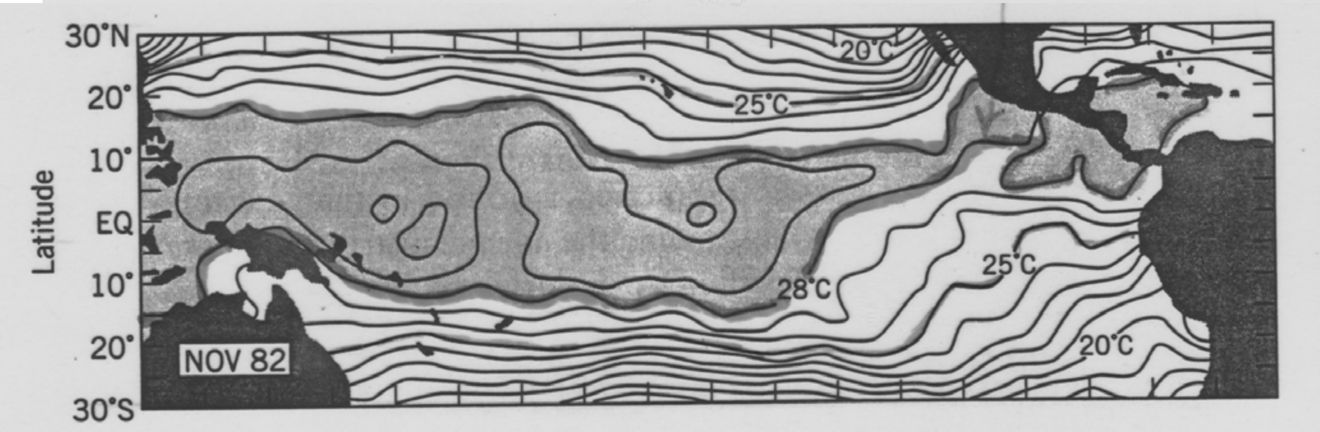


El Nino
Nov 1982

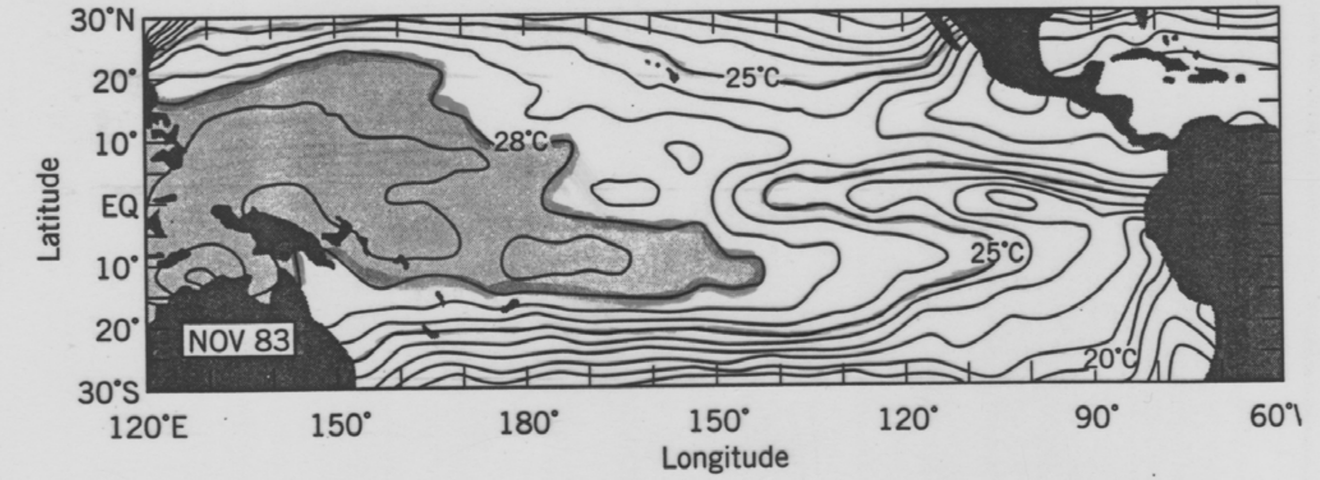


La Nina
Nov 1983

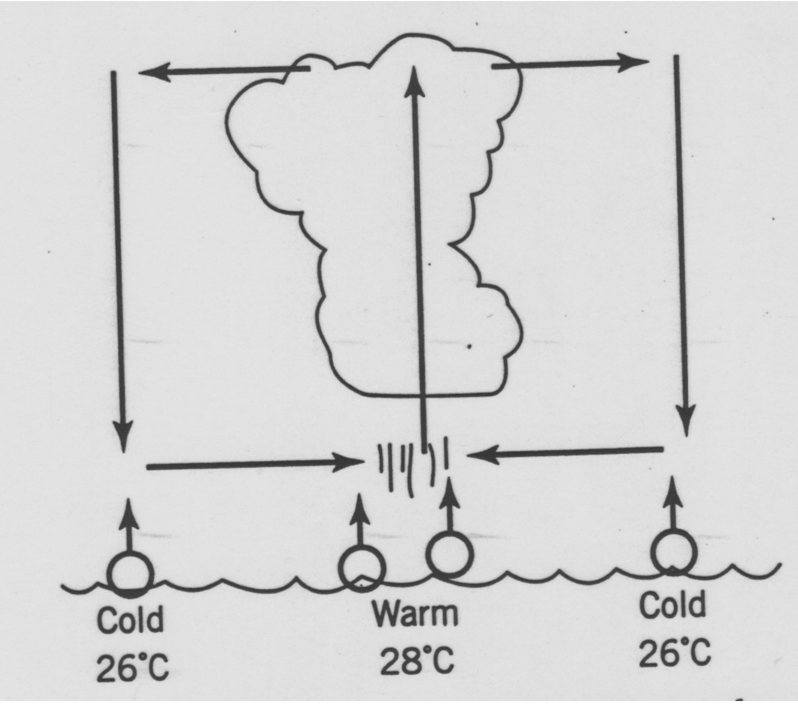


During El Nino, warm SSTs near the Date Line encourage thunderstorms to grow.

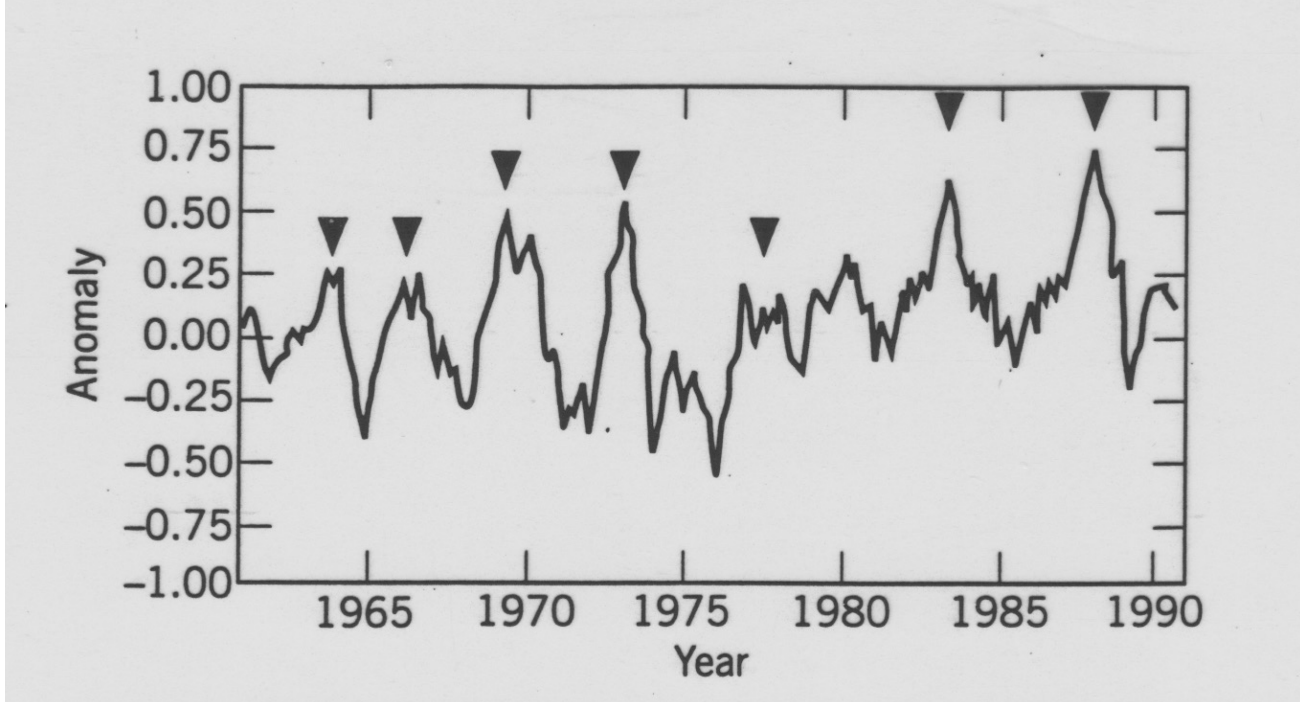


El Nino causes the global average temperature to be warmer.

ENSO modulates tropical deep convection, which affects the long-wave pattern in the extratropics.

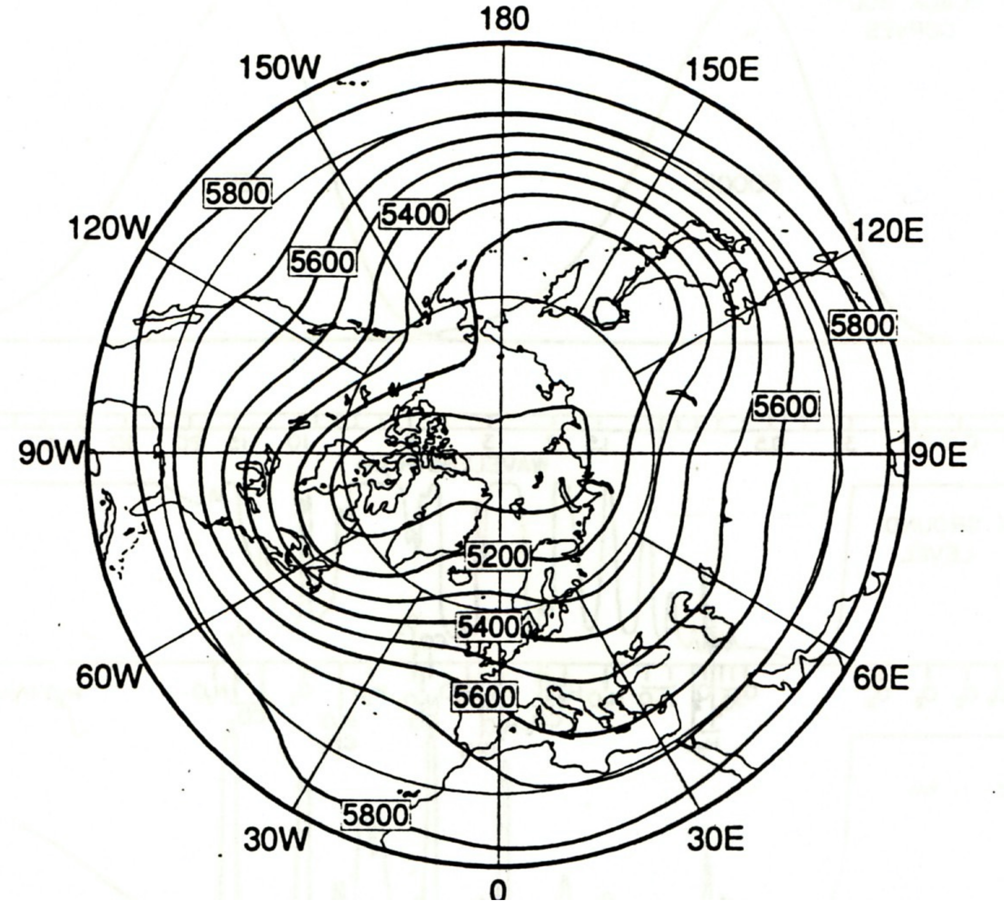


Figure 2.7. A Northern Hemisphere polar stereographic chart of 500 hPa geopotential height averaged for DJF, contour interval 100 m.

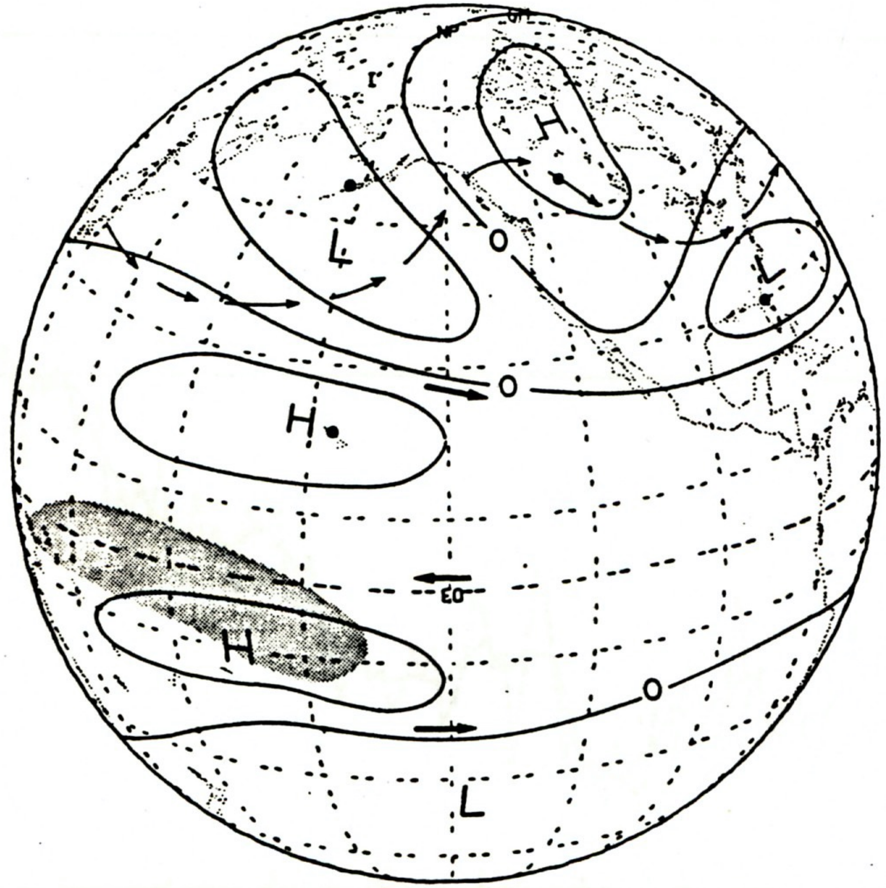


Figure 2.8. Upper tropospheric height anomaly pattern excited by El Nino [Horel and Wallace 1978].

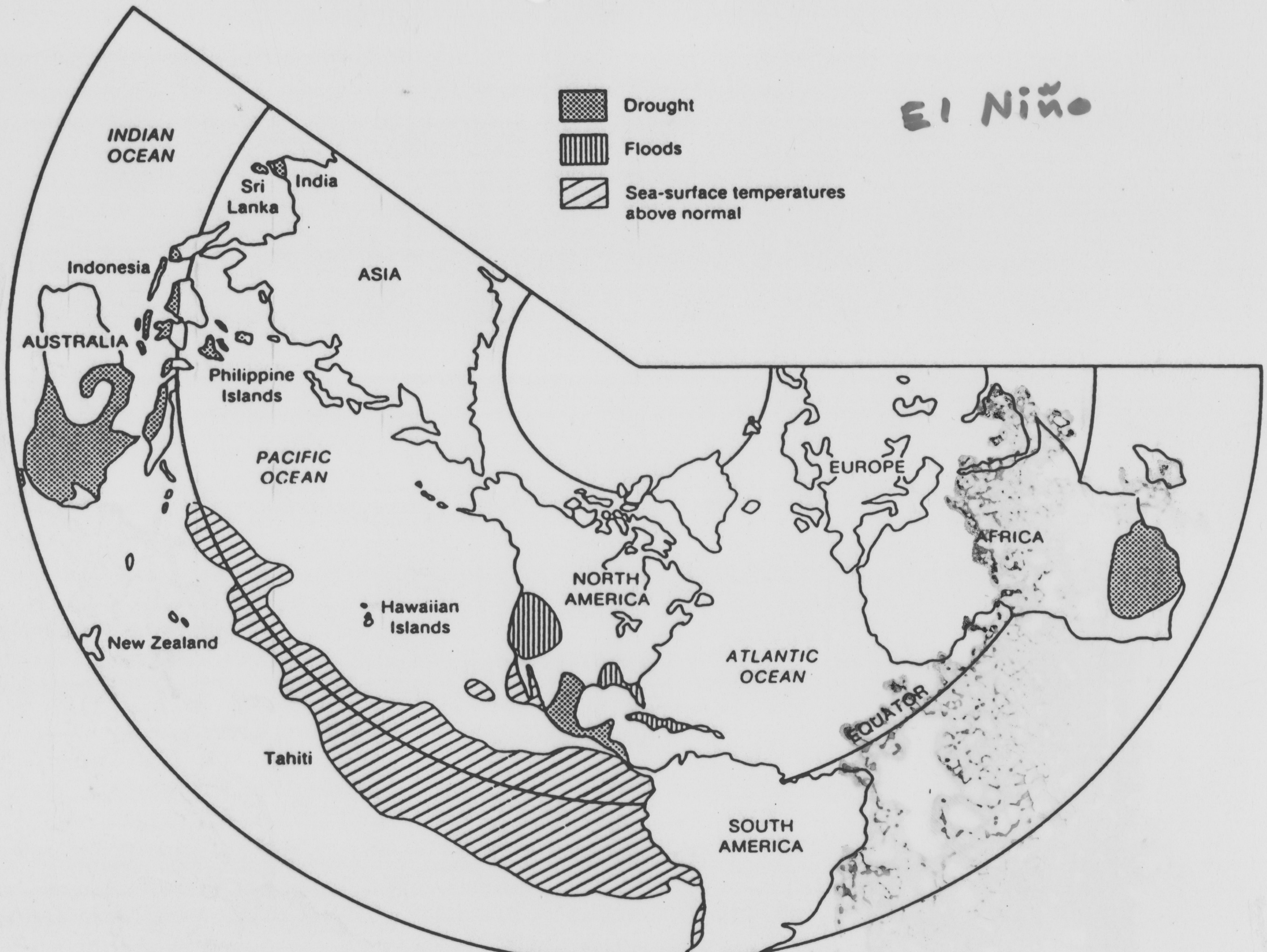


<u>ENSO influences</u>

Droughts – fire, famine

Deluges – tropical disease

Crops

Fisheries

Table 8.8

Major ENSO Events Since 1780

| El Niño | Strength | Regions Affected by Drought/Famine |
|---|---|---|
| 1782–83 | s | China, India |
| 1790–93 | vs | India |
| 1803–04 | s+ | India, South Africa |
| 1824–25 | m+ | China, India, South Africa |
| 1828 | vs | South Africa |
| 1837 | m+ | China, India |
| 1844–46 | s | China, Brazil |
| 1867–70 | m+ | China, India |
| 1873–74 | m | India |
| 1876–78 | vs | China, India, South Africa, Egypt, Java, Brazil |
| 1887–89 | m+ | China, Ethiopia, Sudan, Sahel |
| 1891 | vs | China, India, Brazil |
| 1896–97 | m+ | India, Brazil |
| 1899–1900 | vs | China, India, South Africa |
| 1901–02 | m+ | China, South Africa |
| 1911–13 | s | China, India, Brazil |
| 1917–19 | s | China, India, Brazil, Morocco |
| 1925–26 | vs | China (floods), India |
| 1957–58 | s | China, Brazil |
| 1965–66 | s | China, India |
| 1972–73 | s | China, India, Ethiopia, Sahel, Brazil |
| 1982–83 | vs | China, India, Indonesia, South Africa |
| 1991–95 | s | South Africa, East Africa, Mexico |
| 1997–98 | vs | China (+ floods), Indonesia, Brazil |

Key: m=moderate; s=strong; vs=very strong.

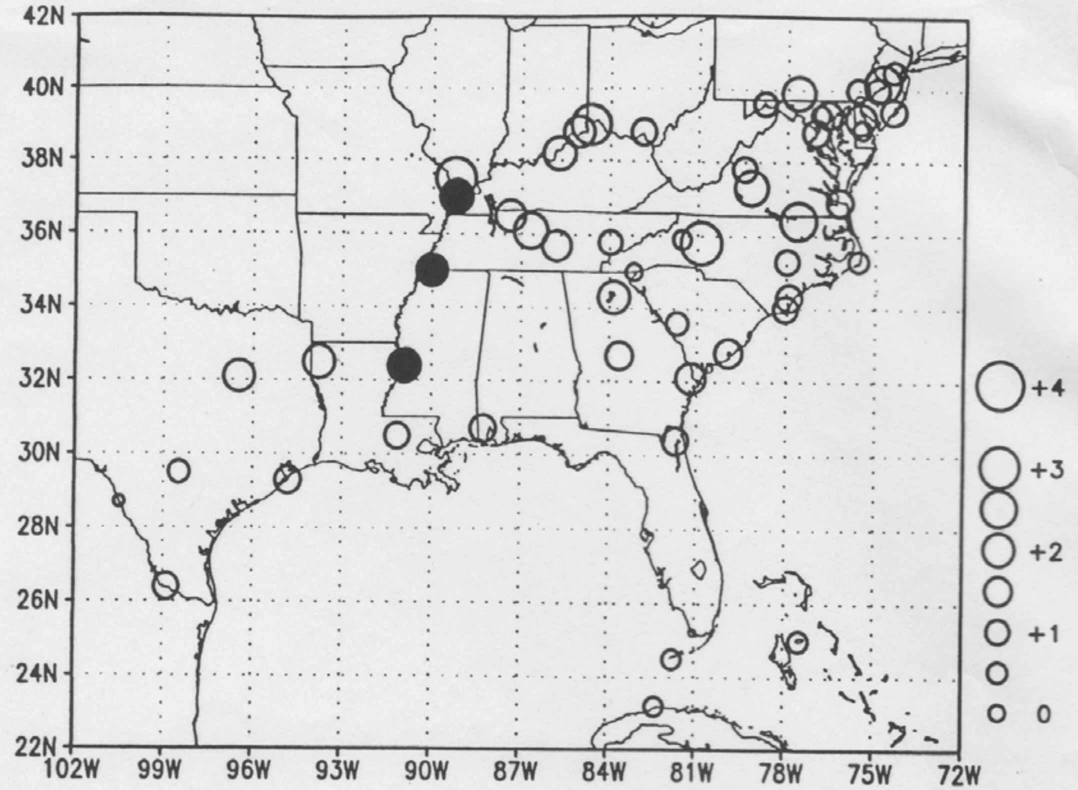


FIG. 3. Map showing temperature departures (°C) from record mean for stations in the southeast United States for the months of February–April of 1878. Magnitude of anomalies is proportional to the size of the circles. Solid dots identify the locations of Cairo, IL, Memphis, TN, and Vicksburg, MS.

TABLE 1. Years with major (> 1000 deaths) yellow fever epidemics, 1793–1905, in the United States. Data taken from Patterson (1993). El Niño years taken from Quinn (1992) and Quinn and Neal (1992).

| Year | Deaths | Main location(s) | El Niño event |
|---|---|---|---|
| 1793 | ca. 5000 | Philadelphia | Yes |
| 1797 | > 1300 | Philadelphia | Yes |
| 1802–03 | > 1000 | Charleston to New York | Yes |
| 1817 | > 1000 | Charleston, New Orleans | Yes |
| 1837–39 | > 1500 | Galveston to Charleston | Yes |
| 1847–49 | > 4000 | mostly in New Orleans | No |
| 1852–55 | > 15 000 | Galveston to Charleston* | Yes |
| 1876 | 1200 | Savannah | No |
| 1878 | ca. 20 000 | Memphis, New Orleans | Yes |

*Greatest death toll occurred in New Orleans with about 15 000 deaths reported.

Increased rainfall and tropical diseases in the southeastern U.S. are more likely during El Nino.

*Bushfire burning in Victoria. The energy of all the fires on Black Saturday was the equivalent of fifteen hundred Hiroshimas.*

El Nino

February 7, 2009

"Black Saturday"
fire near
Melbourne
Australia

Figure 7.4
Key Stages in the Development of ENSO Theory

| | |
|---|---|
| 1. Recognizing global, synchronized drought | Roxburgh: 1790s<br>Blanford: 1880 |
| 2. Linking drought to interhemispheric atmosphere "see-saw" | Blanford: 1880<br>Lockyer and Lockyer: 1900 |
| 3. Identifying the Southern Oscillation (SO) | Hildebrandsson: 1899<br>Walker: 1920s |
| 4. Unifying the SO and El Niño in a single model | Bjerknes: 1960s |
| 5. Recognizing La Niña (ENSO cold phase) | Philander: 1980s |
| 6. Mechanism for the phase transition | Wyrtki: 1980s |
| 7. Successful predictive model | Cane and Zebiak: 1986 |
| 8. Nature of interdecadal fluctuations | ?? |

MEI = Weighted spatial patterns of 6 variables (SLP, SST, U, V, T, clouds)
monthly averages + = warm phase (El Nino) – = cold phase (La Nina)

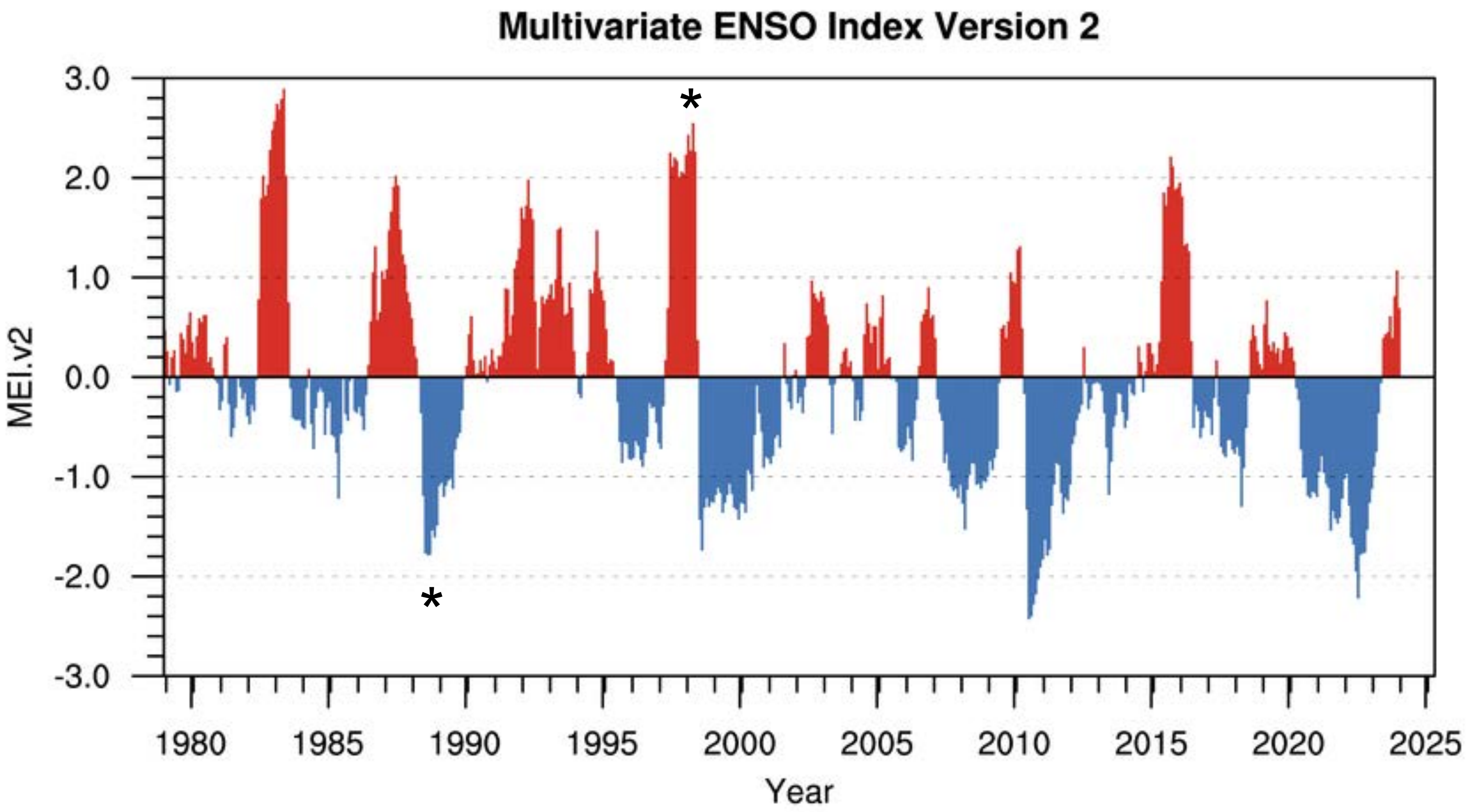

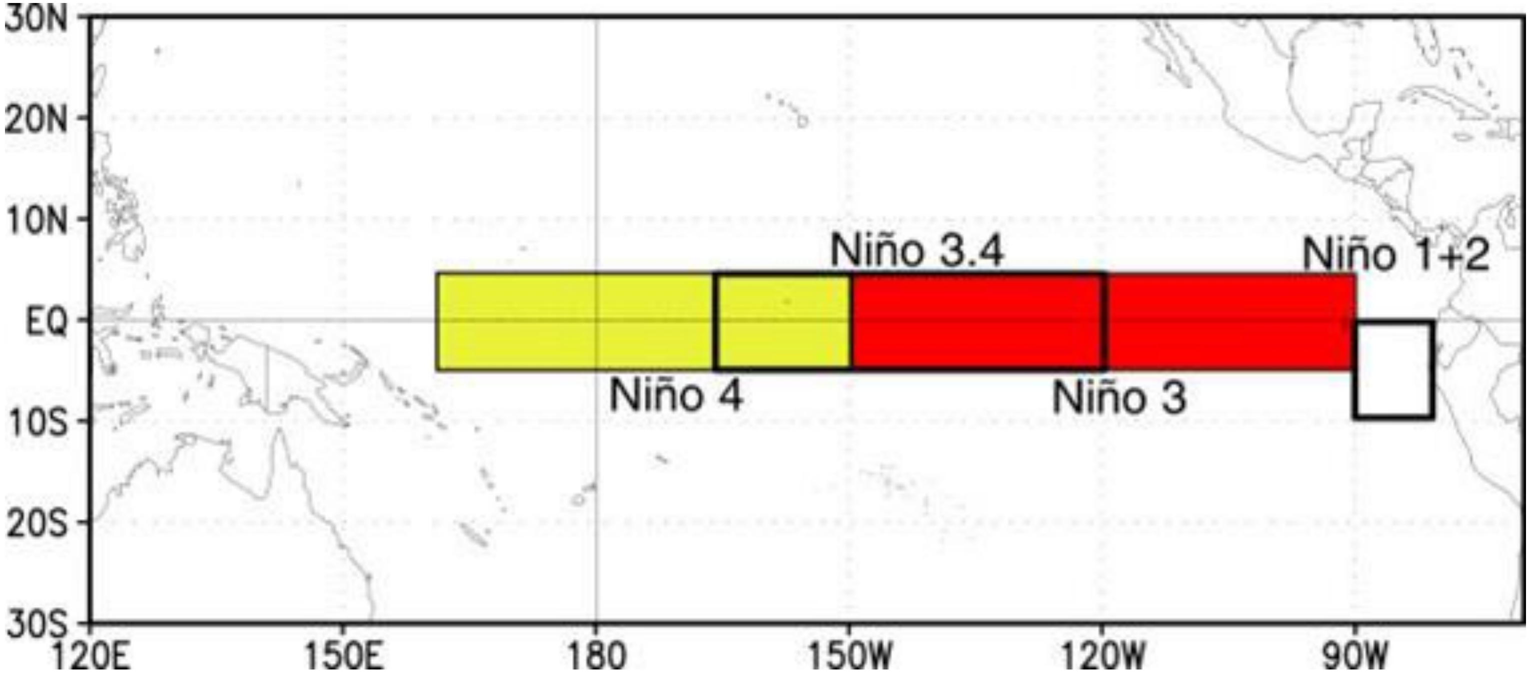

30N
20N
10N
EQ
10S
20S
30S
120E
150E
180
150W
120W
90W
Niño 3.4
Niño 1+2
Niño 4
Niño 3

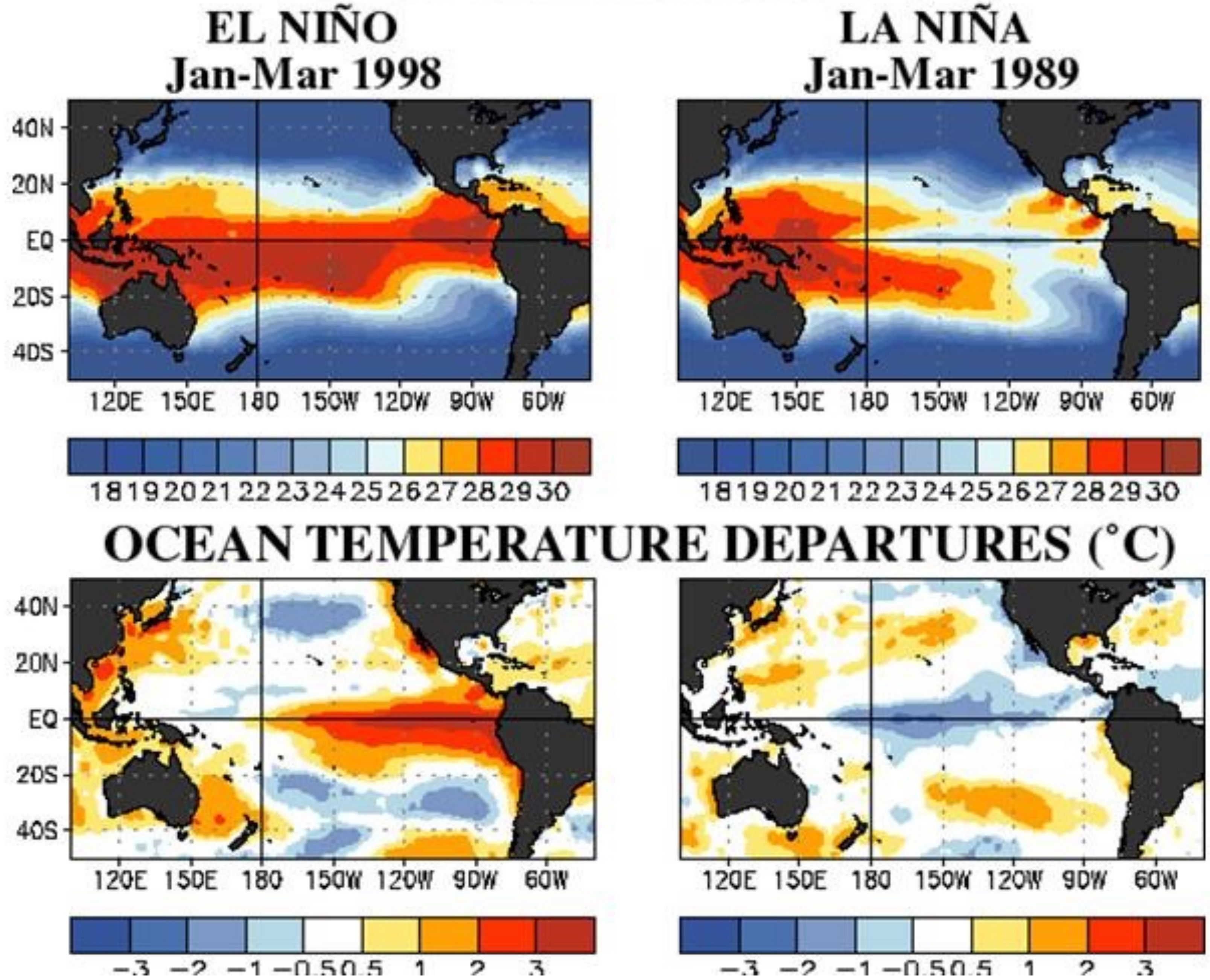


Figure 3.19. Sea surface temperature and anomaly for the 1998 El Nino and the 1989 La Nina [www.cpc.noaa.gov].

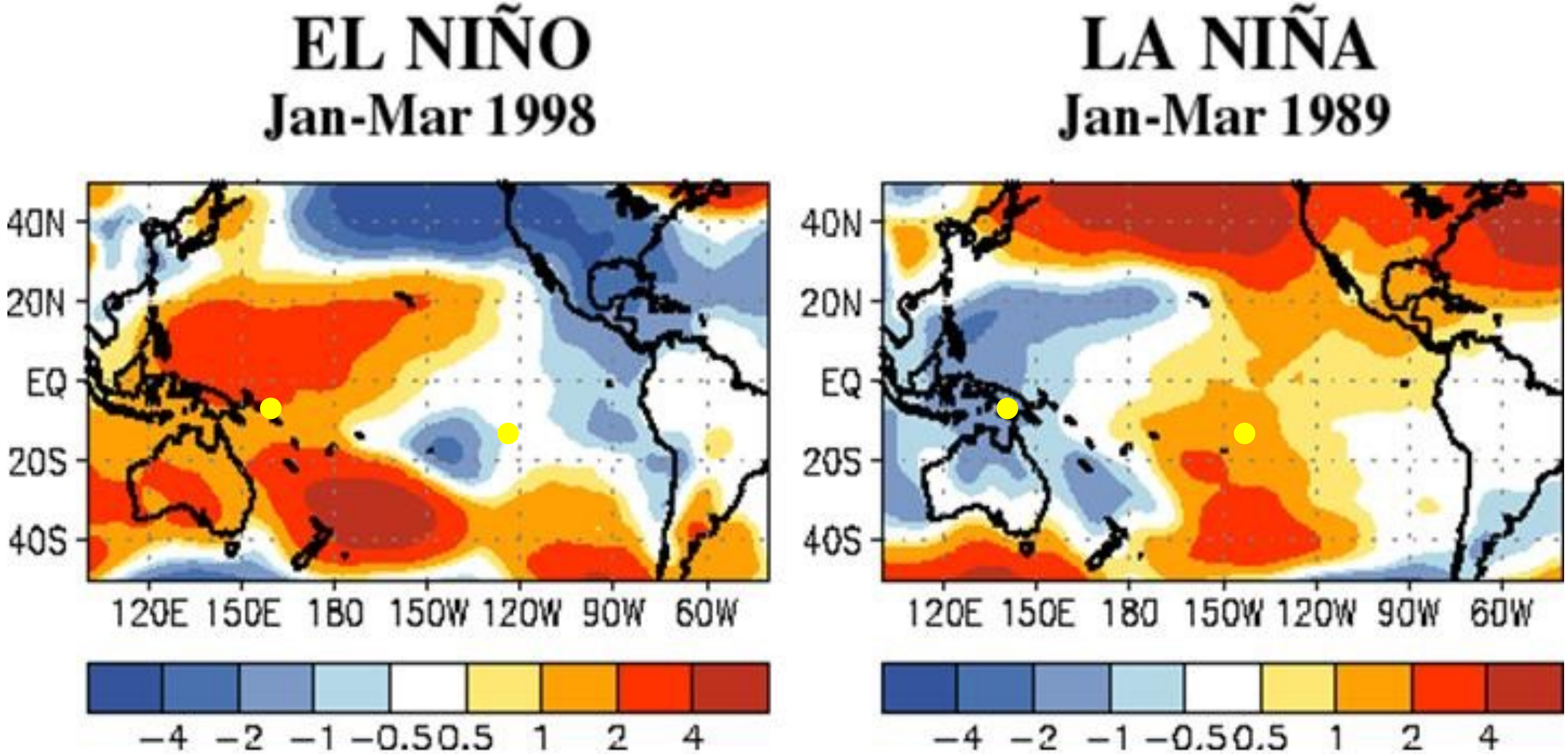


Figure 3.20. Sea level pressure anomalies for the 1998 El Nino and the 1989 La Nina [www.cpc.noaa.gov]. Yellow dots indicate the locations of Darwin and Tahiti.

# El Nino

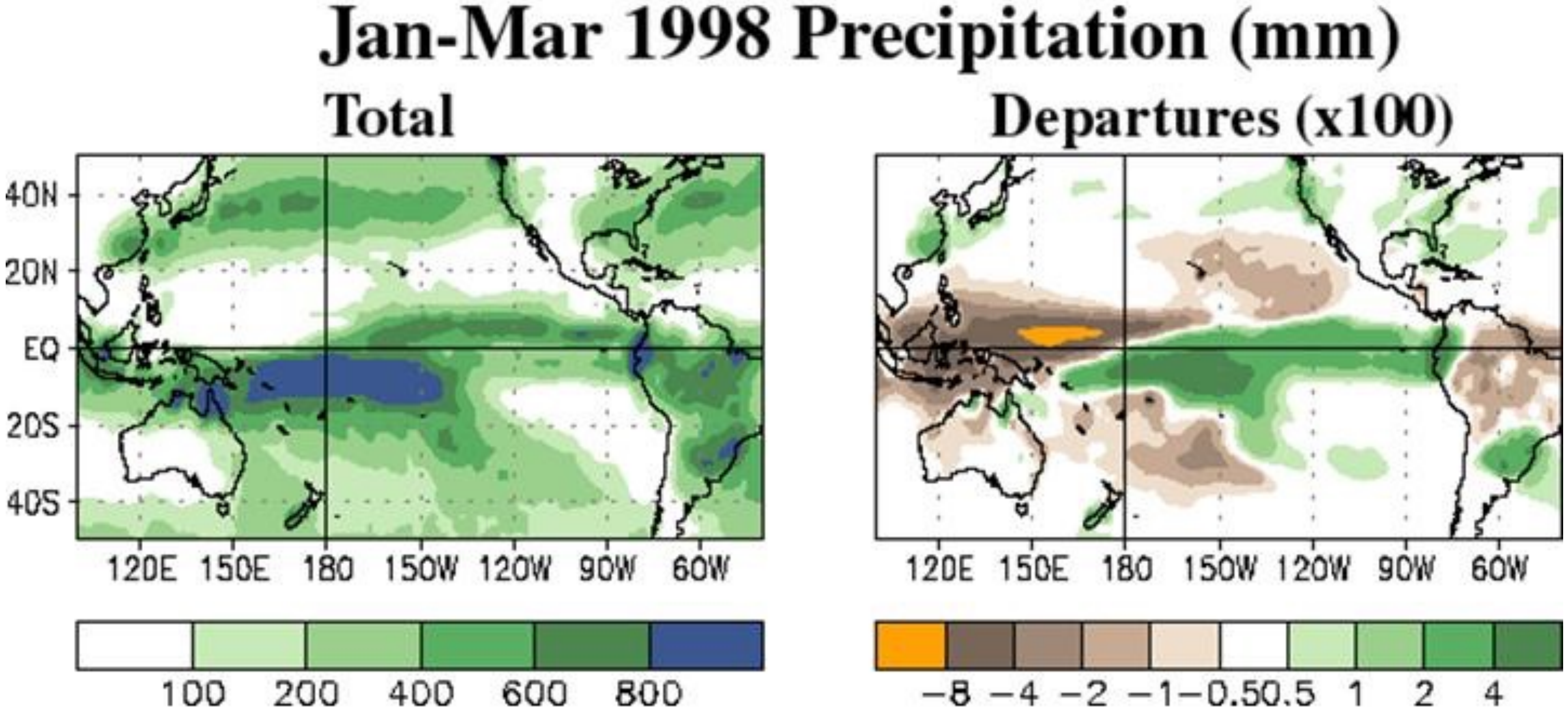


Figure 3.22a. January-March rainfall and rainfall anomaly during the 1998 El Nino.

# La Nina

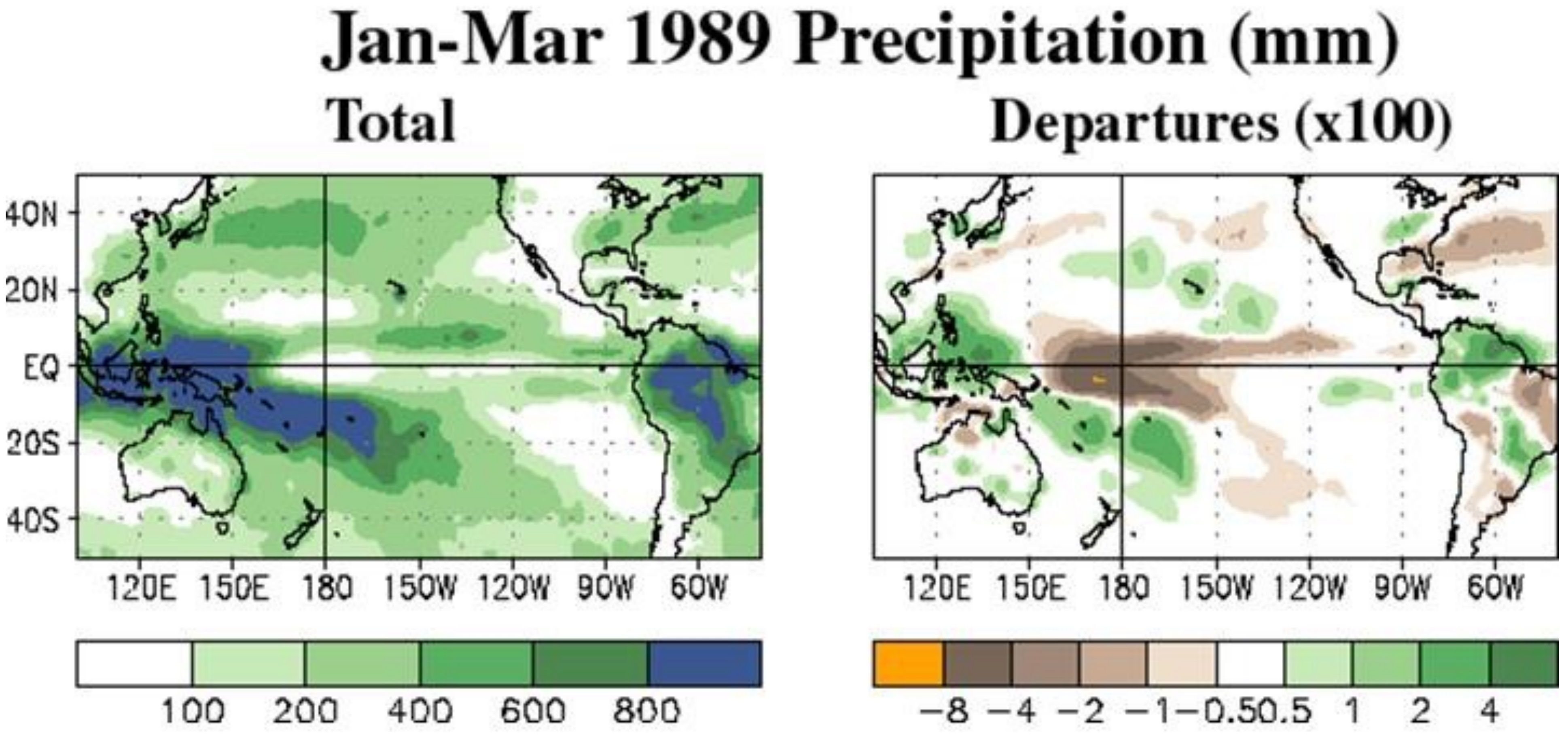


Figure 3.22b. January-March rainfall and anomaly during the 1989 La Nina.

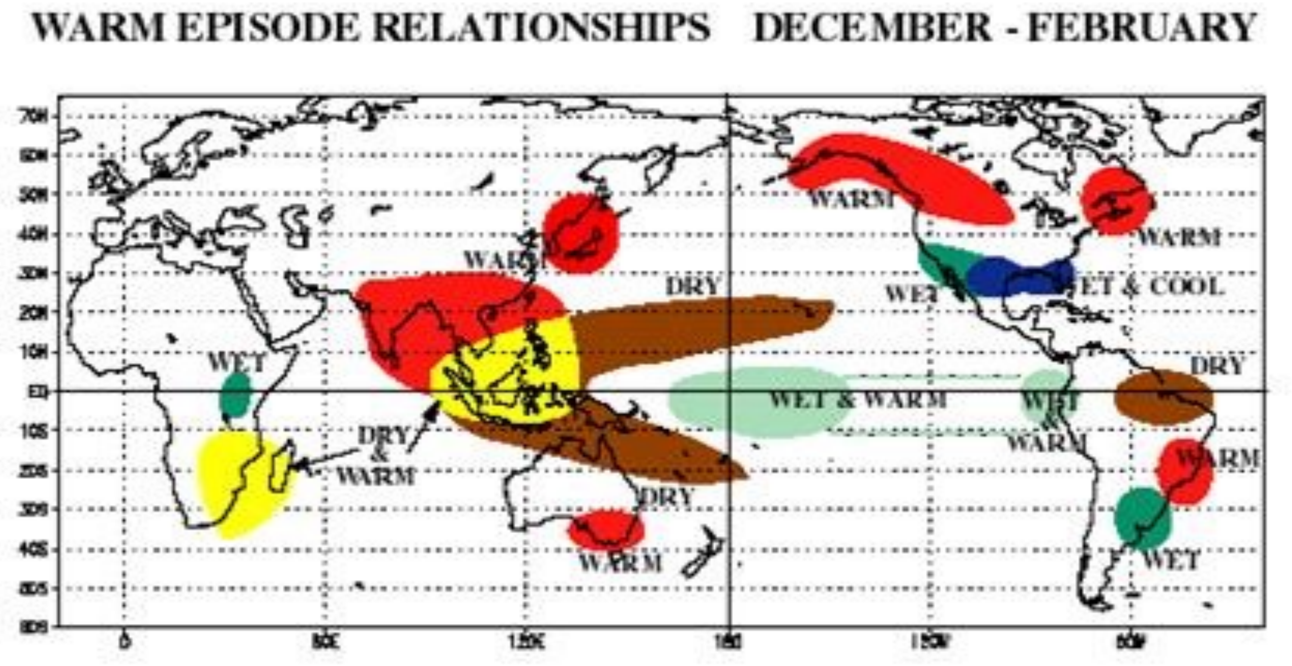


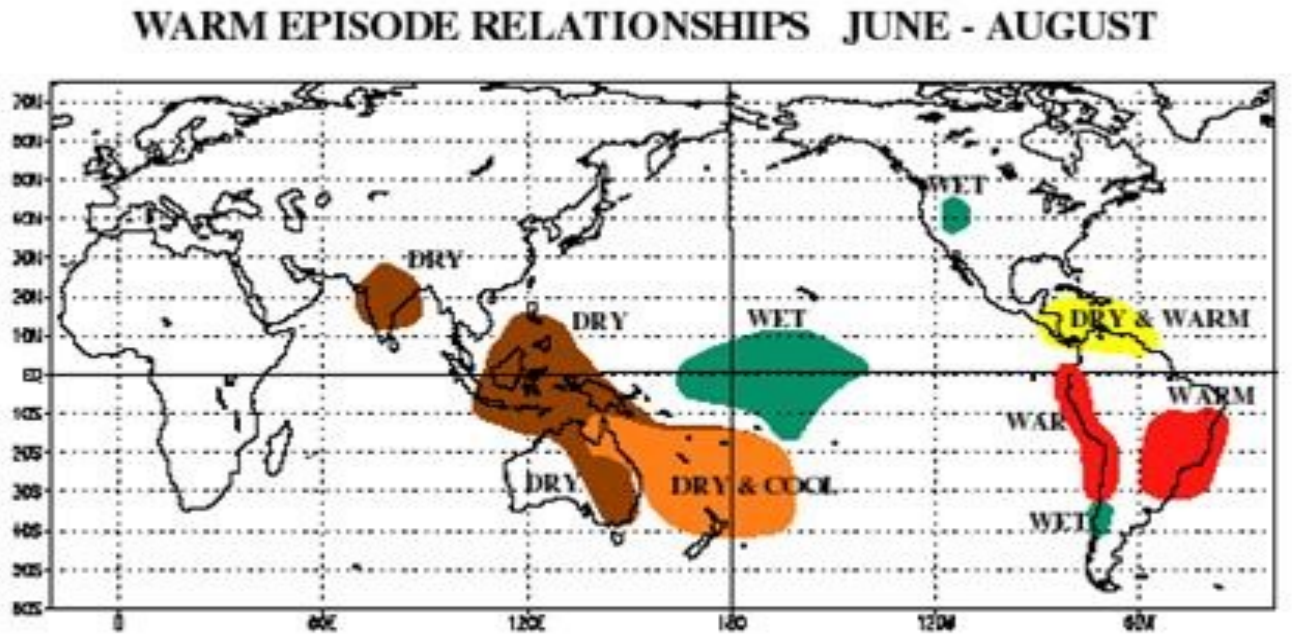


# El Nino

Figure 3.23a. Global weather relationships for DJF and JJA which tend to occur during El Nino [www.cpc.noaa.gov].

COLD EPISODE RELATIONSHIPS DECEMBER - FEBRUARY

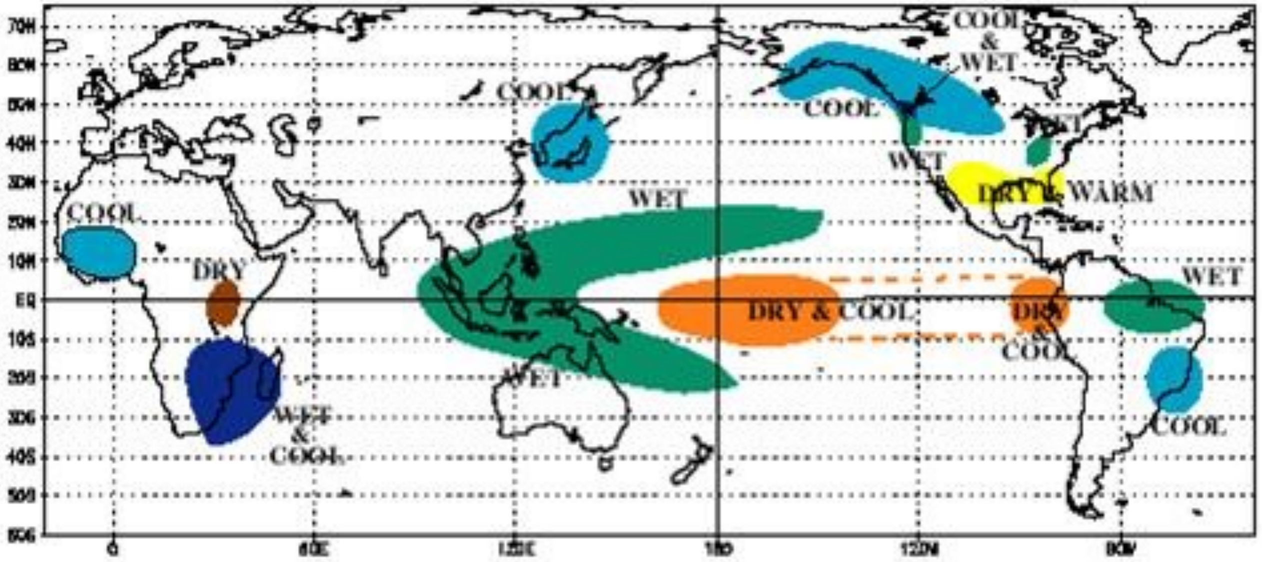


COLD EPISODE RELATIONSHIPS JUNE - AUGUST

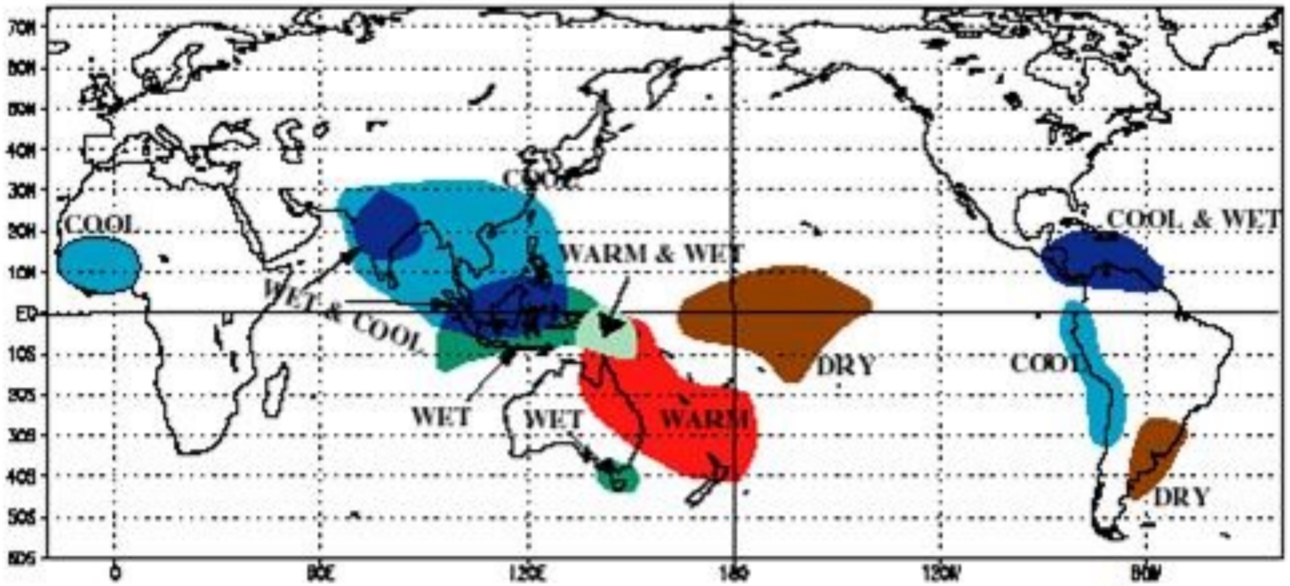


Chaco Canyon 1120

# La Nina

Figure 3.23b. Global weather relationships for DJF and JJA which tend to occur during La Nina [www.cpc.noaa.gov].

What’s been happening with ENSO lately?

1. “The Blob” 2013-2018
   El Nino / Modoku 2015-2016

2. La Nina 2020 – 2023

3. El Nino 2023 - 2024

MEI = Weighted spatial patterns of 6 variables (SLP, SST, U, V, T, clouds)
monthly averages + = warm phase (El Nino) – = cold phase (La Nina)

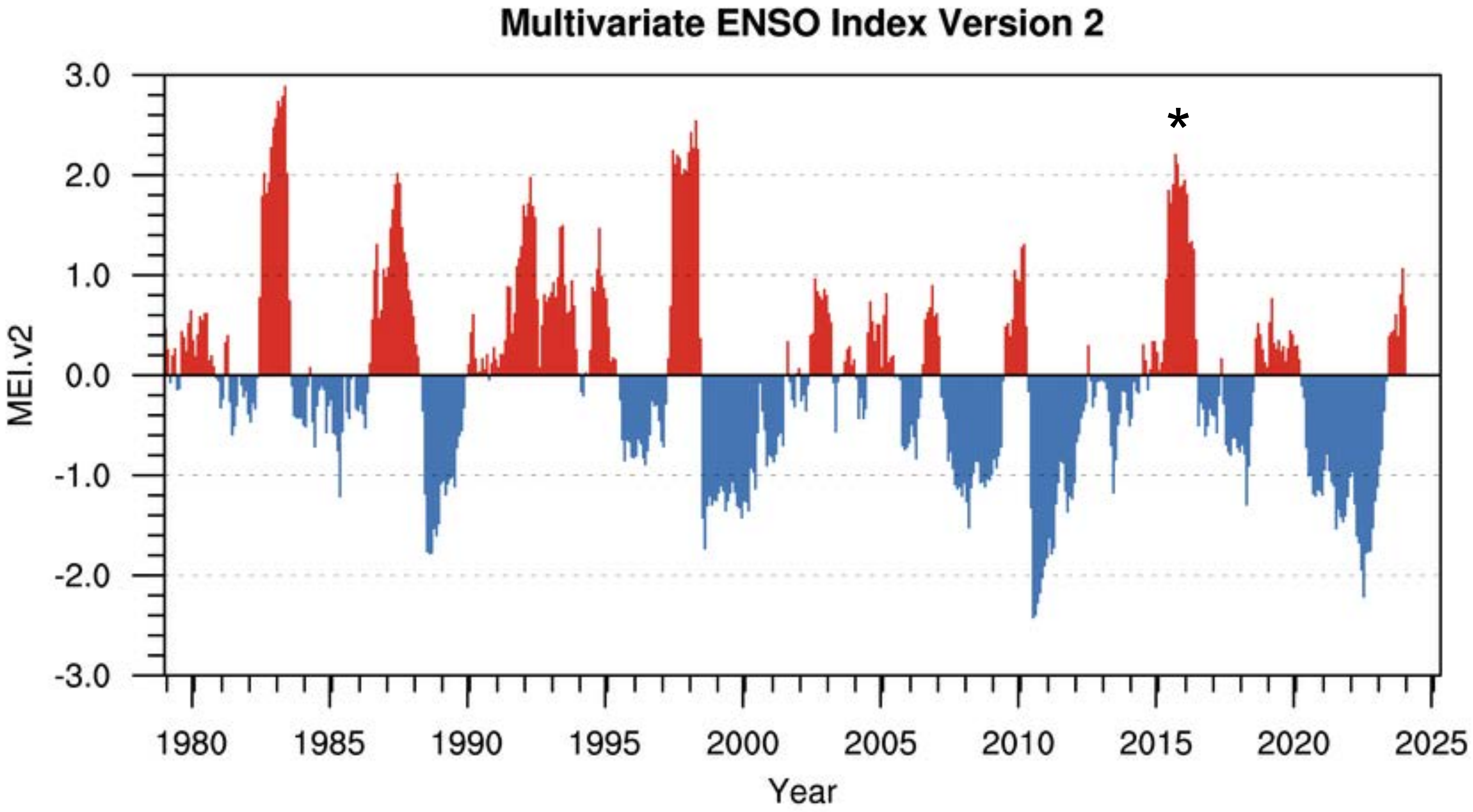

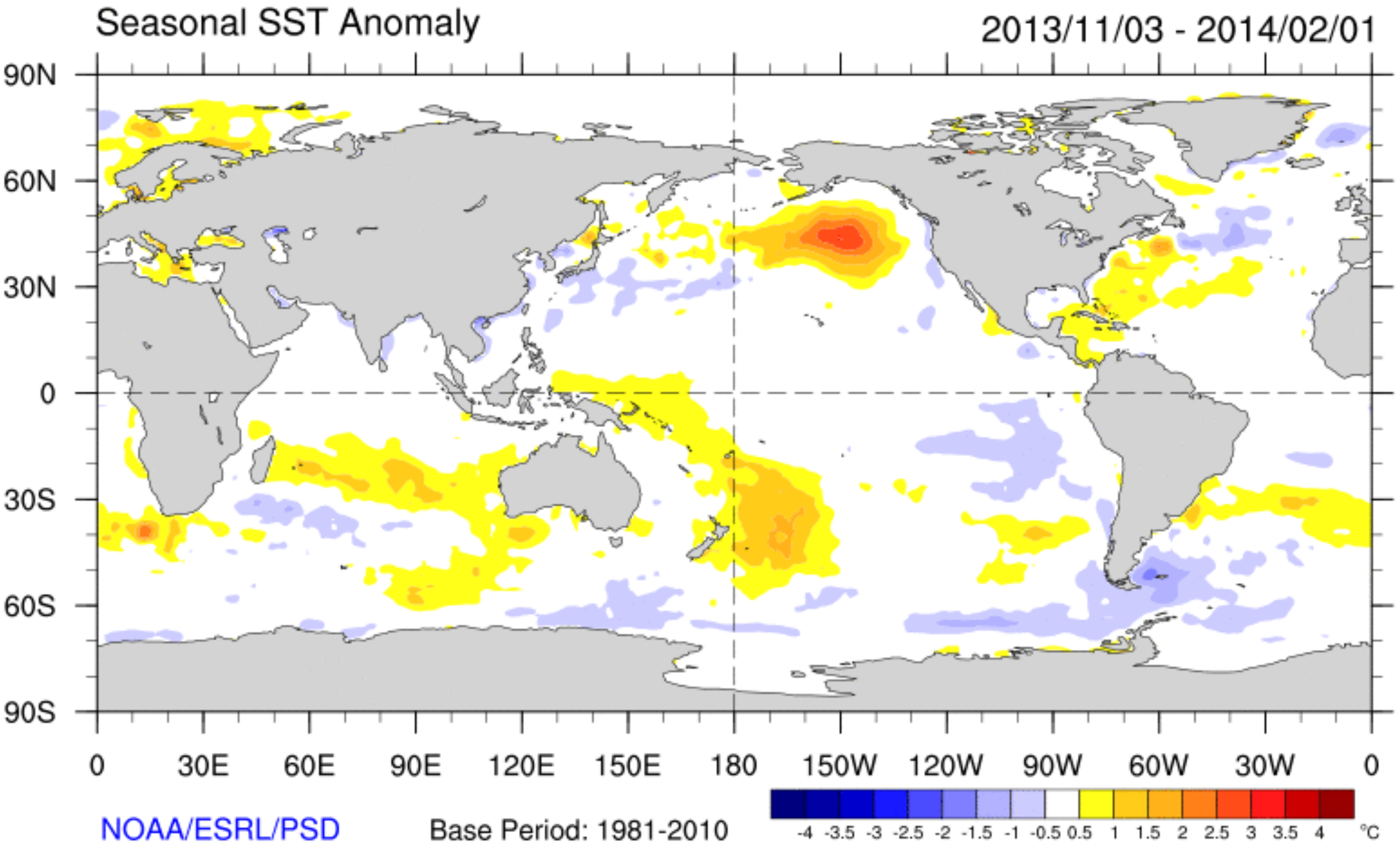
Seasonal SST Anomaly
2013/11/03 - 2014/02/01
90N
60N
30N
0
30S
60S
90S
0
30E
60E
90E
120E
150E
180
150W
120W
90W
60W
30W
0
-4 -3.5 -3 -2.5 -2 -1.5 -1 -0.5 0.5 1 1.5 2 2.5 3 3.5 4
°C
NOAA/ESRL/PSD
Base Period: 1981-2010

“The Blob” helped create an extension of the polar vortex over North America

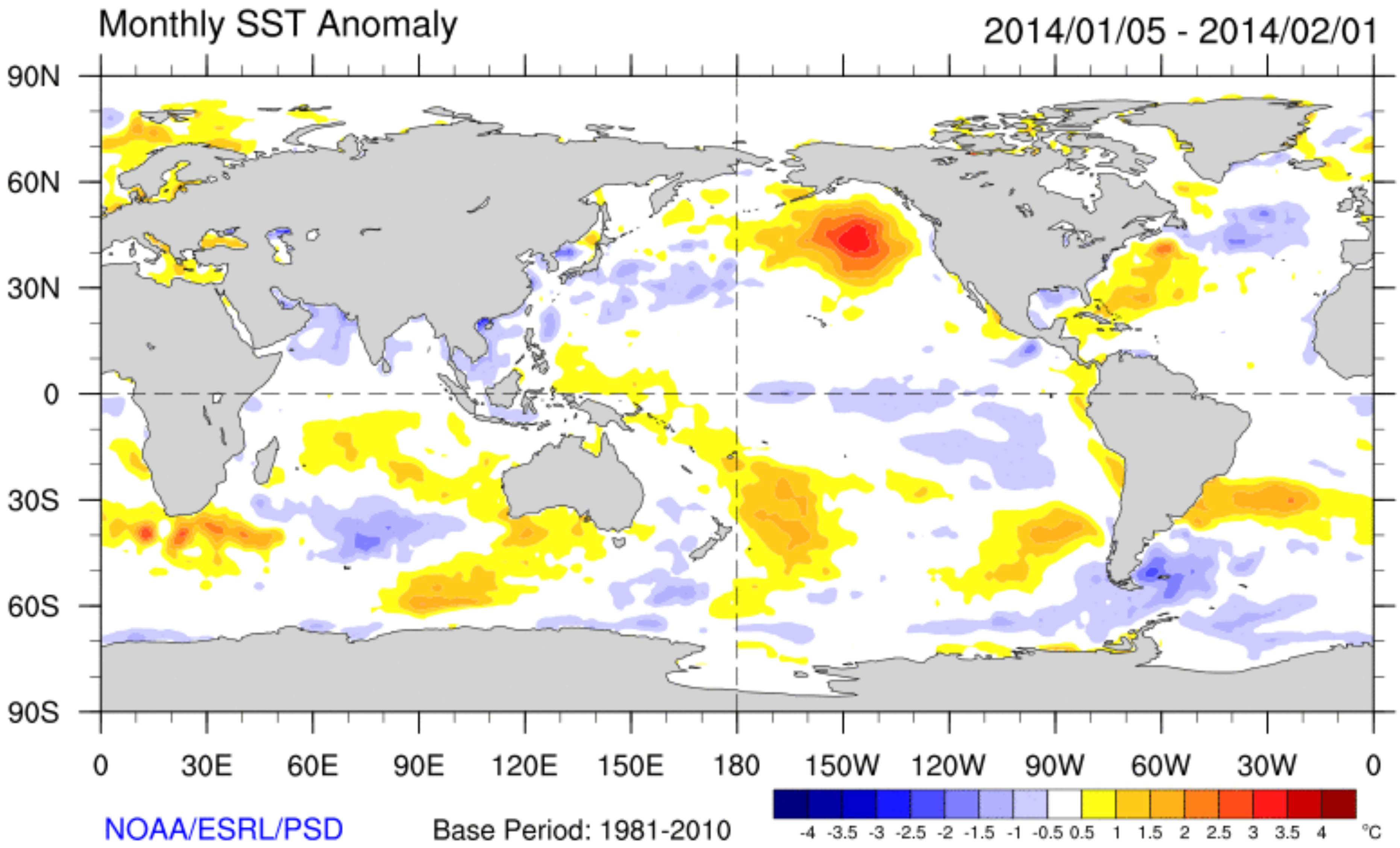

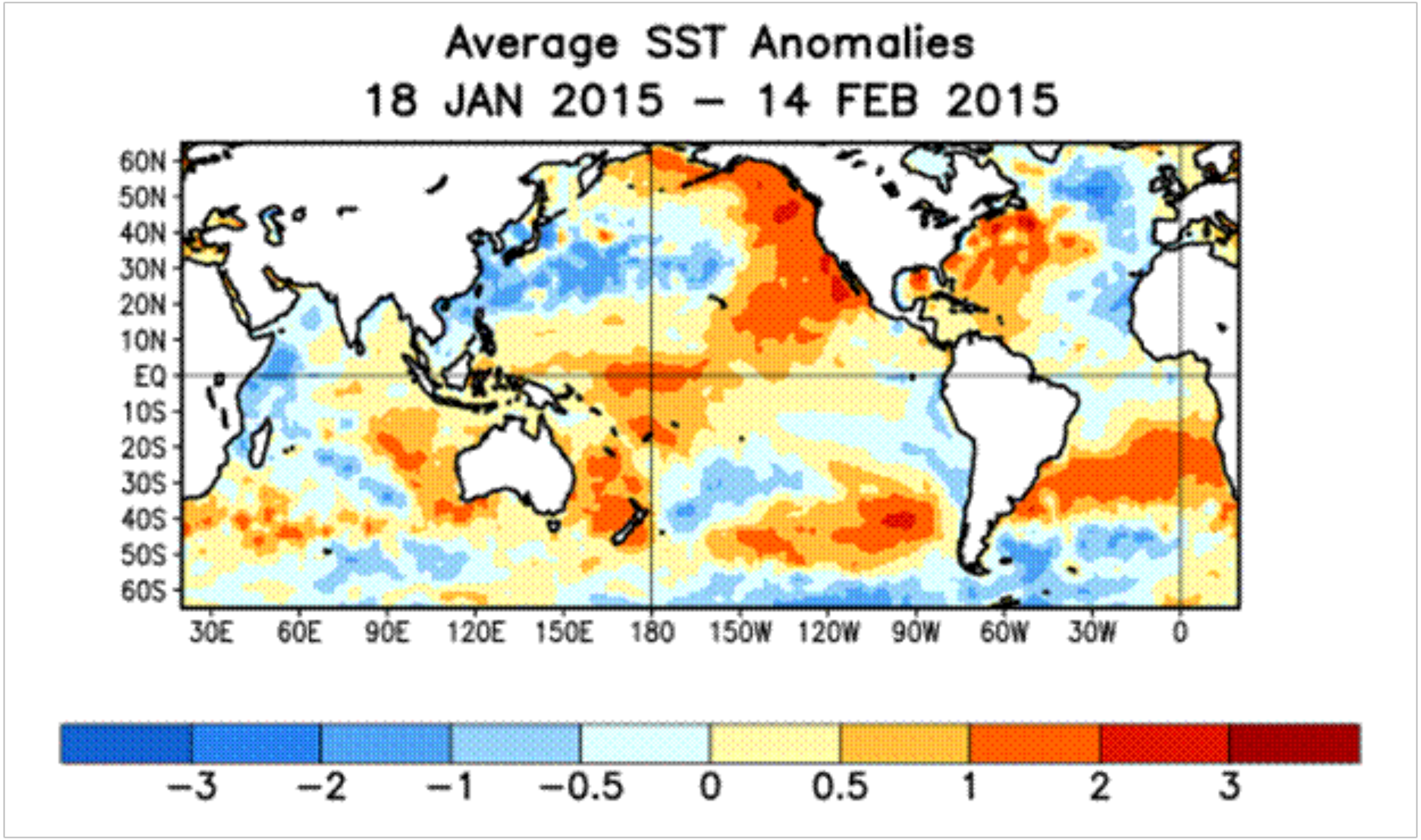
Average SST Anomalies
18 JAN 2015 – 14 FEB 2015
60N
50N
40N
30N
20N
10N
EQ
10S
20S
30S
40S
50S
60S
30E
60E
90E
120E
150E
180
150W
120W
90W
60W
30W
0
−3
−2
−1
−0.5
0
0.5
1
2
3

“Modoki”

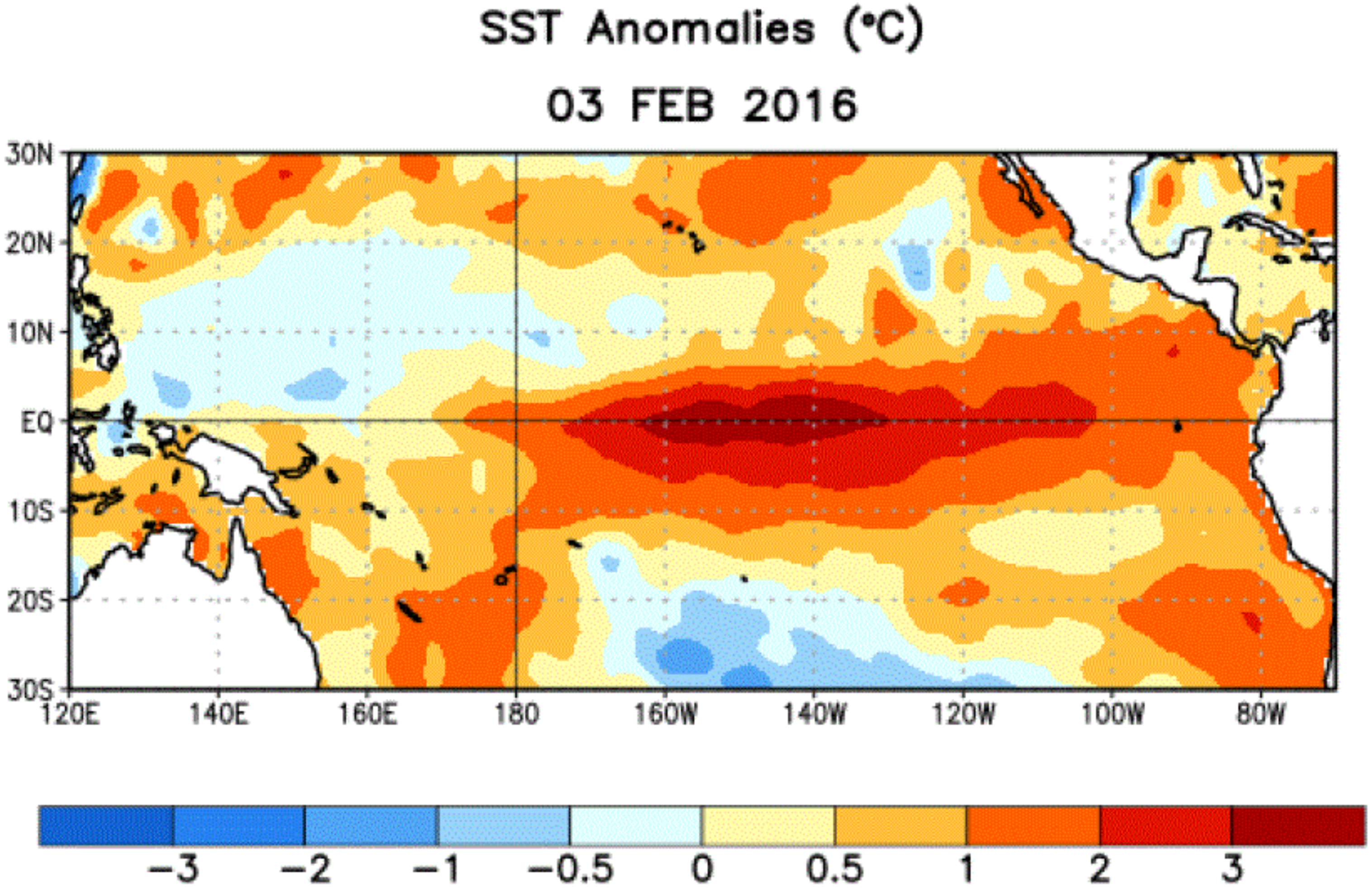


Figure 1. Average sea surface temperature (SST) anomalies (°C) for the week centered on 3 February 2016. Anomalies are computed with respect to the 1981-2010 base period weekly means.

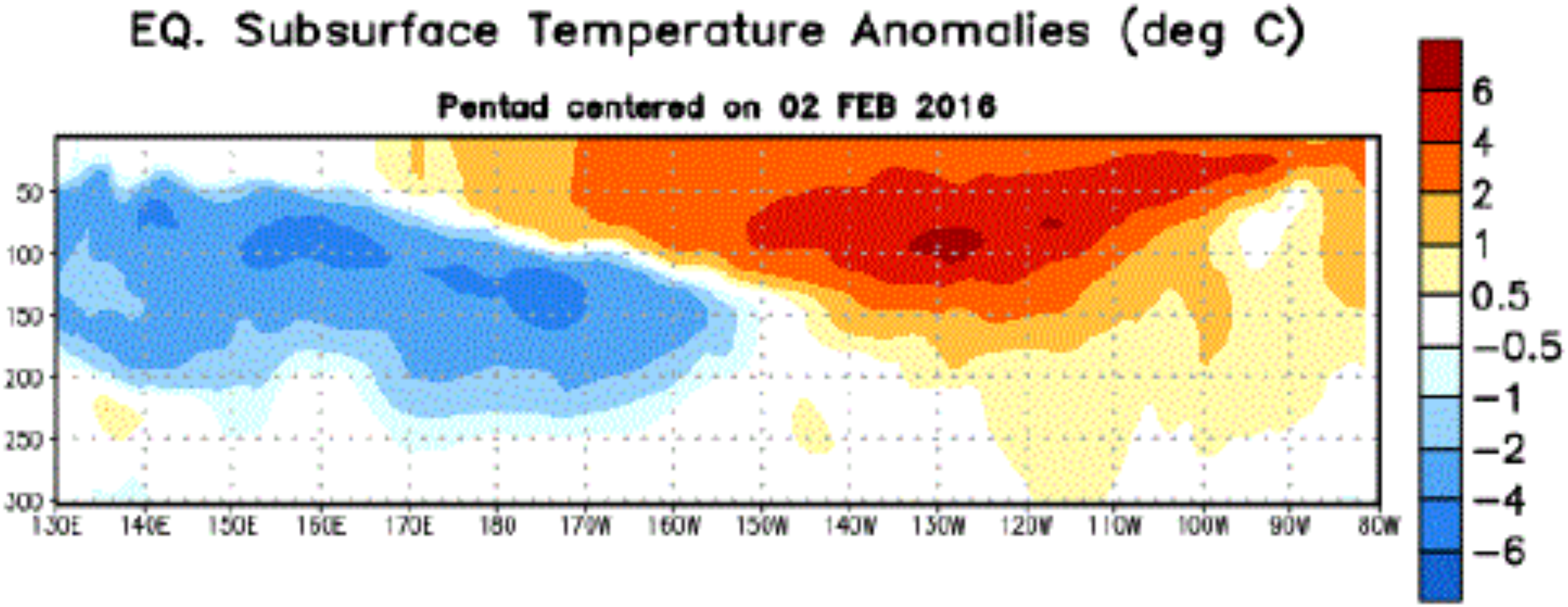


Figure 4. Depth-longitude section of equatorial Pacific upper-ocean (0-300m) temperature anomalies (°C) centered on the pentad of 2 February 2016. The anomalies are averaged between 5°N-5°S. Anomalies are departures from the 1981-2010 base period pentad means.

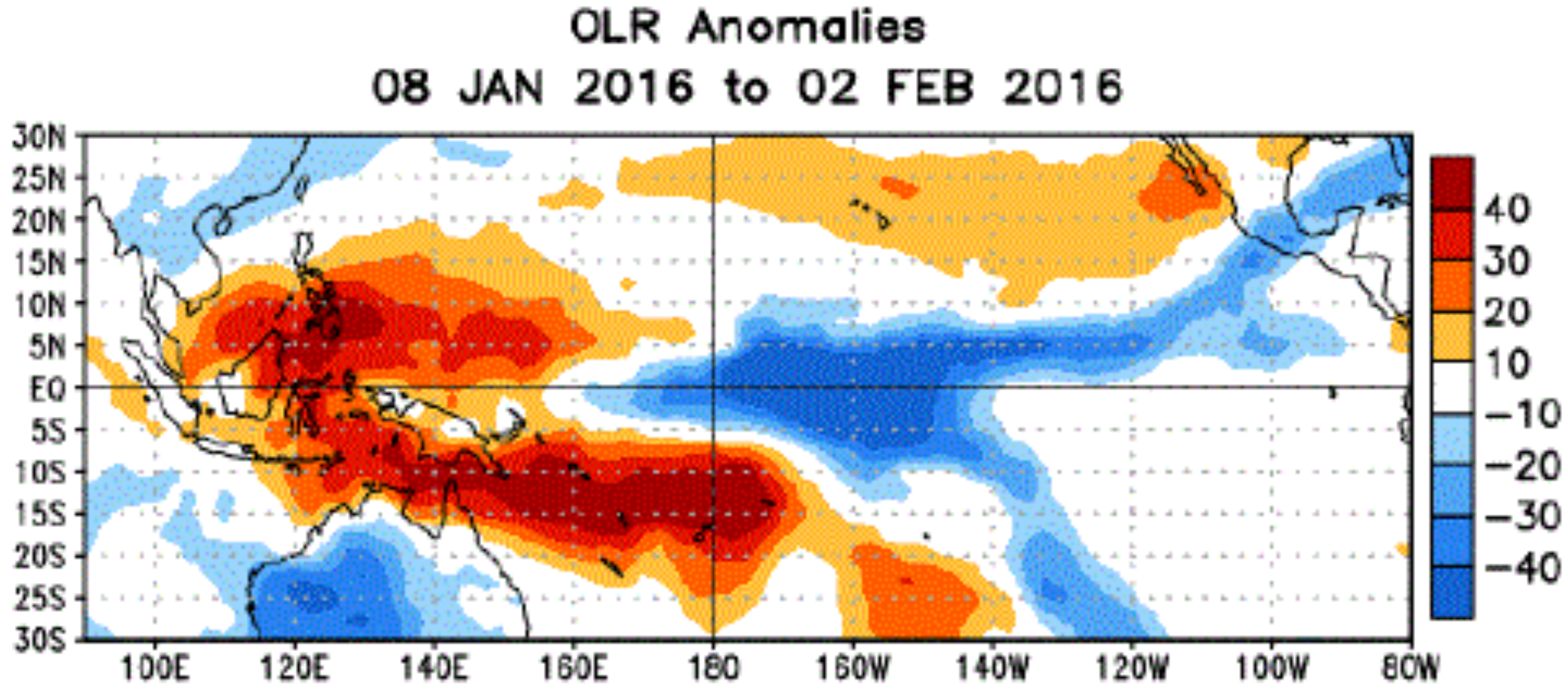


Figure 5. Average outgoing longwave radiation (OLR) anomalies ($W/m^2$) for the period 8 January – 2 February 2016. OLR anomalies are computed as departures from the 1979-1995 base period pentad means.

MEI = Weighted spatial patterns of 6 variables (SLP, SST, U, V, T, clouds)
monthly averages + = warm phase (El Nino) – = cold phase (La Nina)

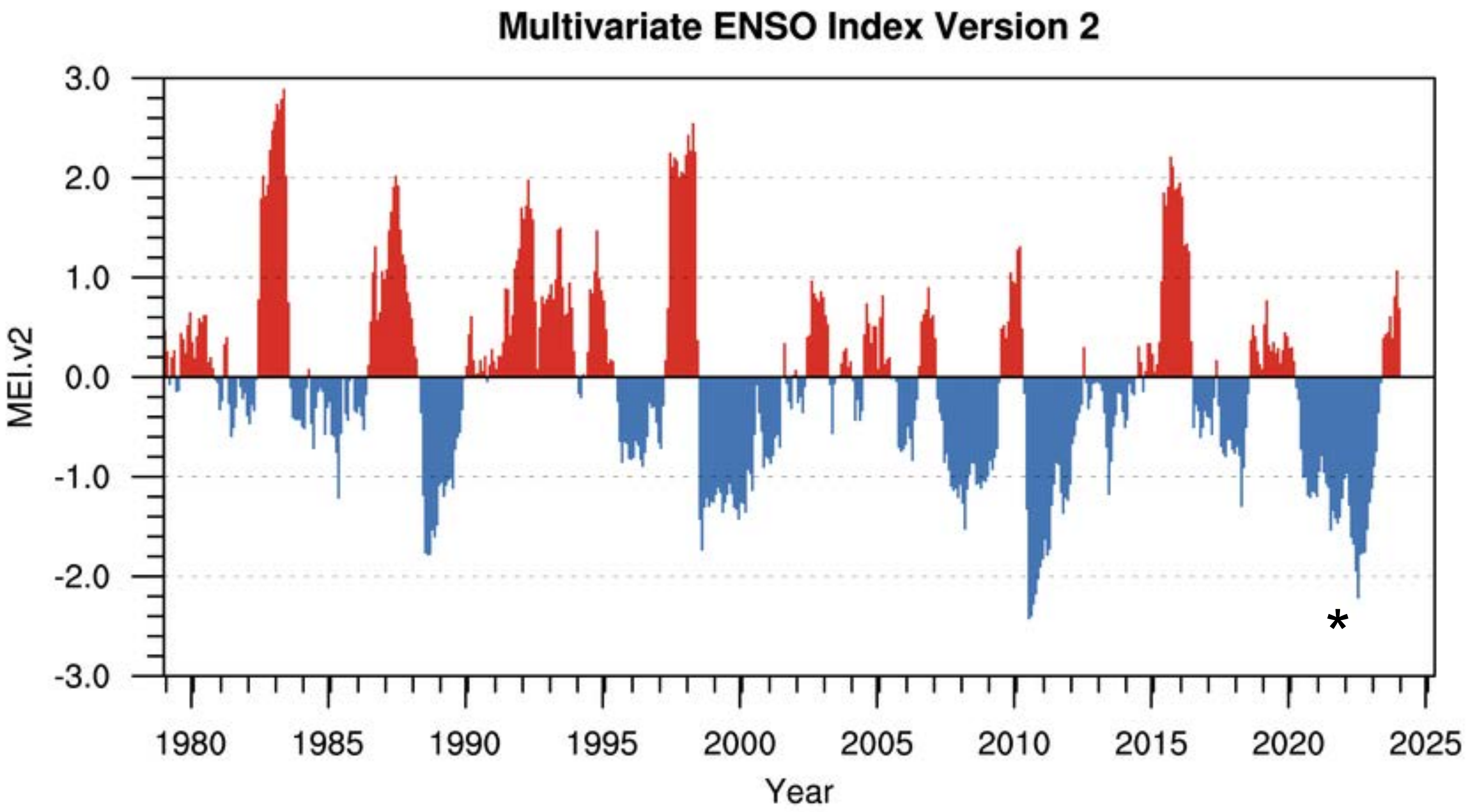

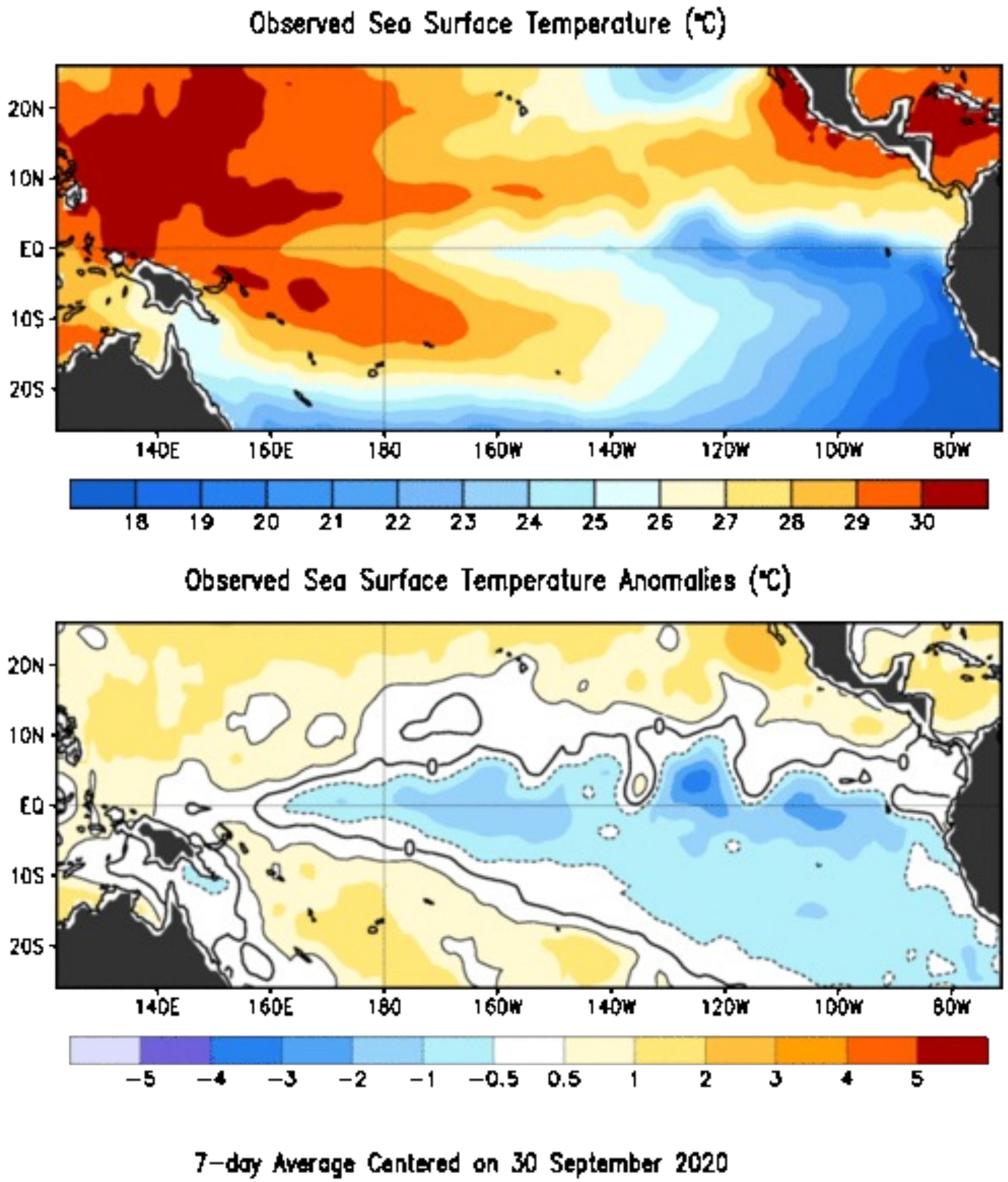


https://www.cpc.ncep.noaa.gov/

## Equatorial T Penatd Anomaly (ºC), Sep 30 2020

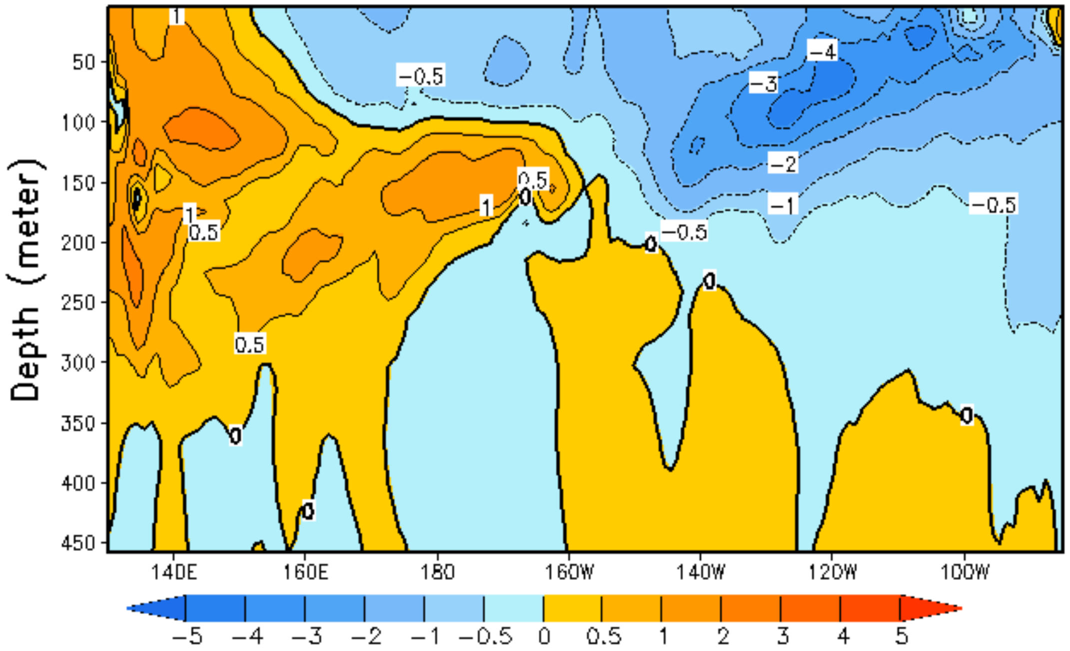


## Equatorial T Penatd Mean (ºC), Sep 30 2020

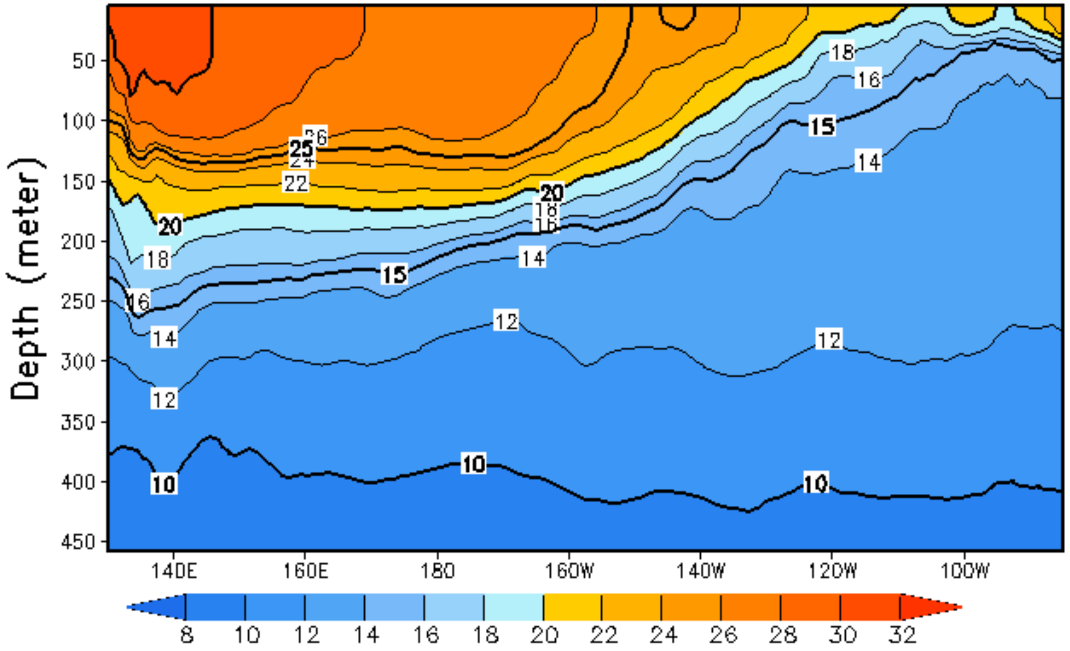

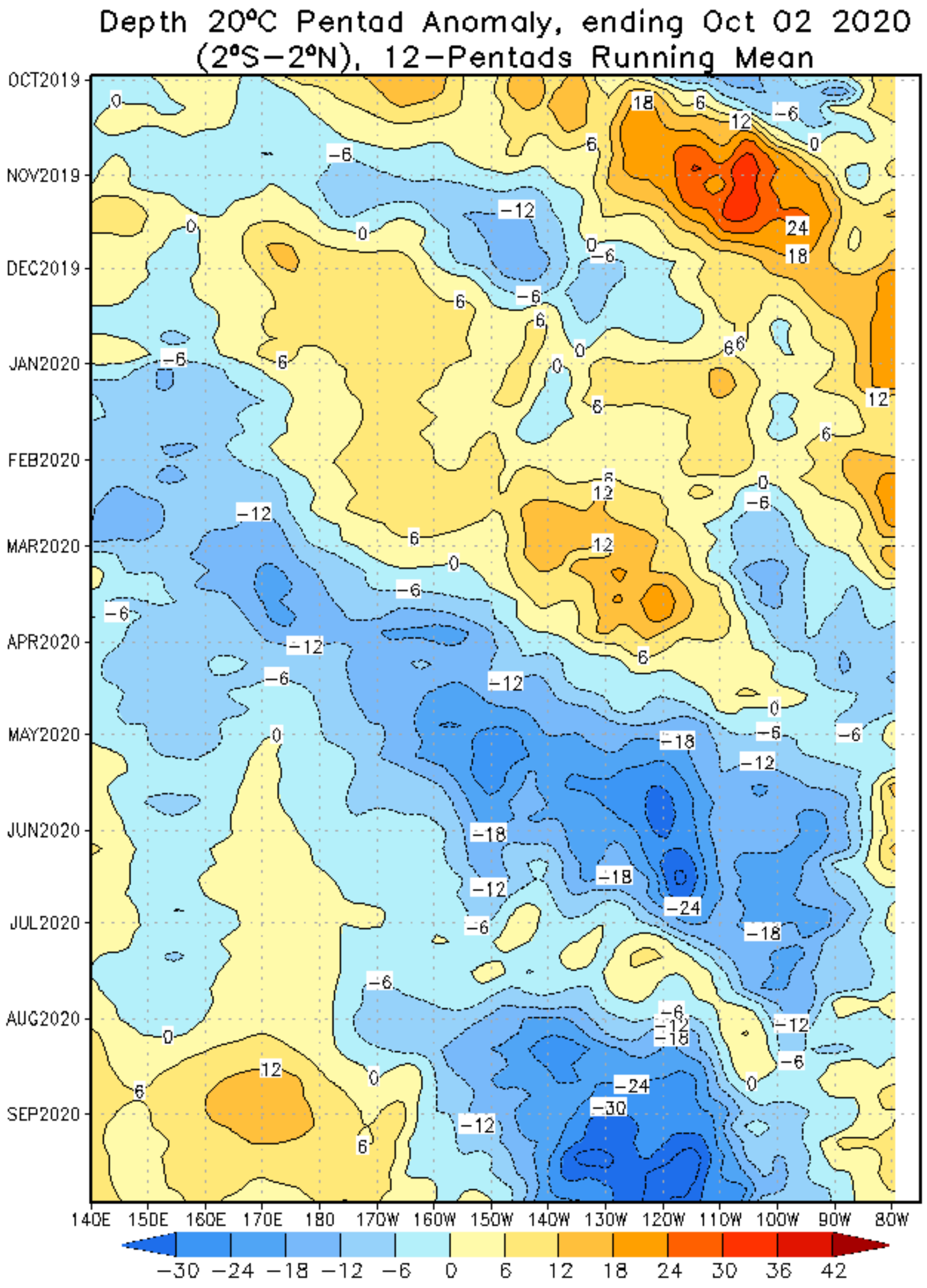


Warm and cold anomalies travel eastward

at the speed of an oceanic Kelvin wave

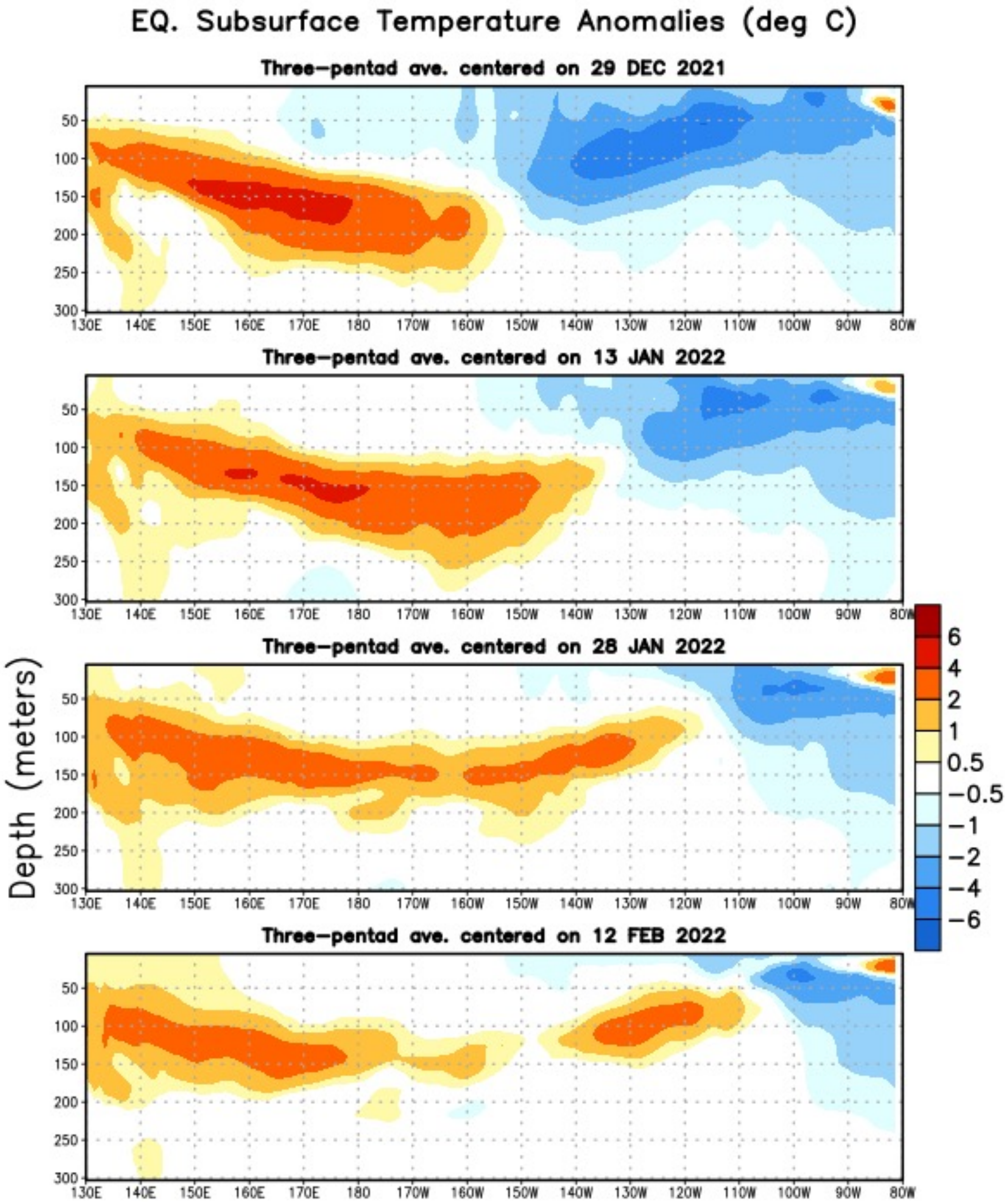
EQ. Subsurface Temperature Anomalies (deg C)
Three-pentad ave. centered on 29 DEC 2021
Three-pentad ave. centered on 13 JAN 2022
Three-pentad ave. centered on 28 JAN 2022
Three-pentad ave. centered on 12 FEB 2022
Depth (meters)
50
100
150
200
250
300
130E
140E
150E
160E
170E
180
170W
160W
150W
140W
130W
120W
110W
100W
90W
80W
6
4
2
1
0.5
−0.5
−1
−2
−4
−6

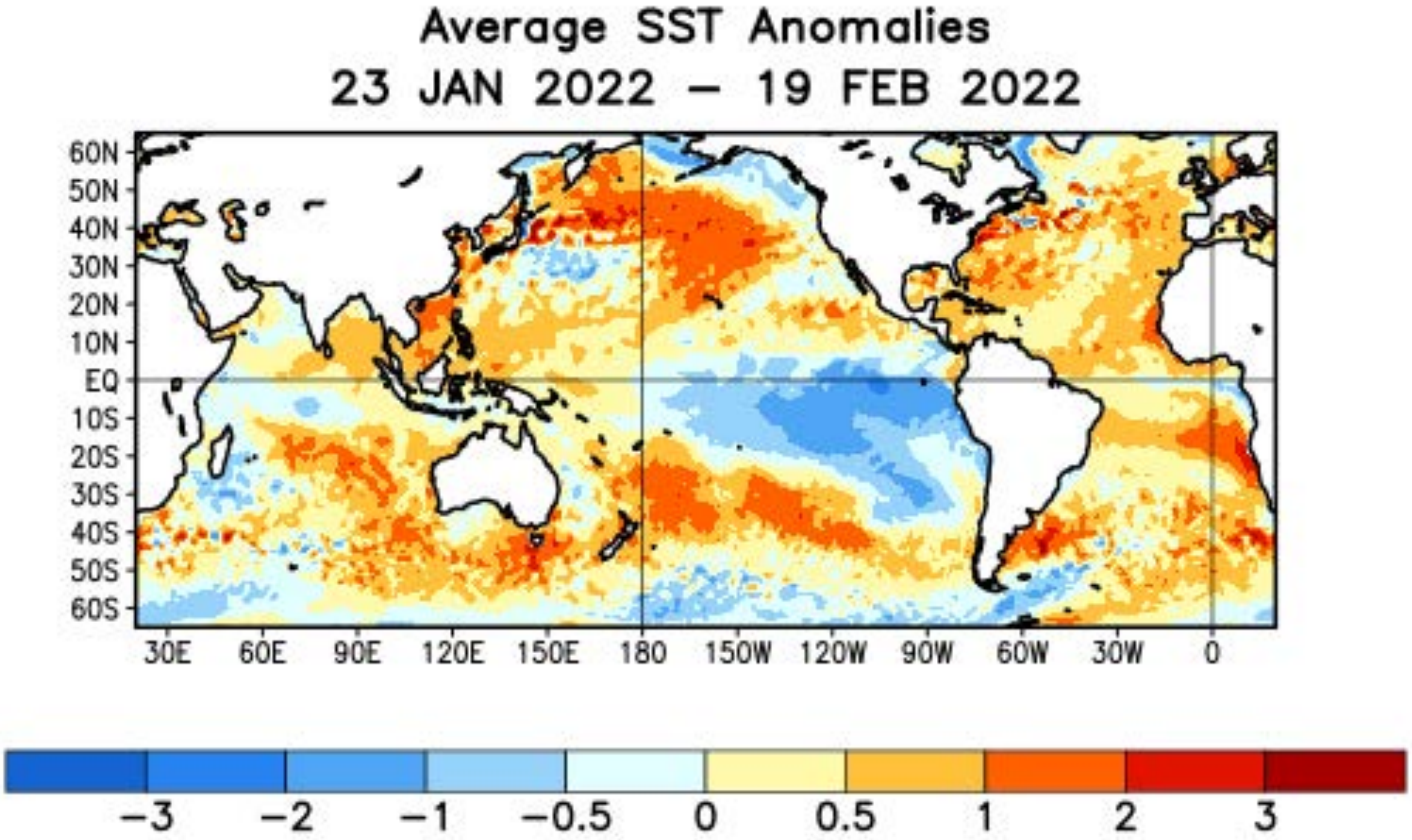
Average SST Anomalies
23 JAN 2022 – 19 FEB 2022
60N
50N
40N
30N
20N
10N
EQ
10S
20S
30S
40S
50S
60S
30E
60E
90E
120E
150E
180
150W
120W
90W
60W
30W
0
−3
−2
−1
−0.5
0
0.5
1
2
3

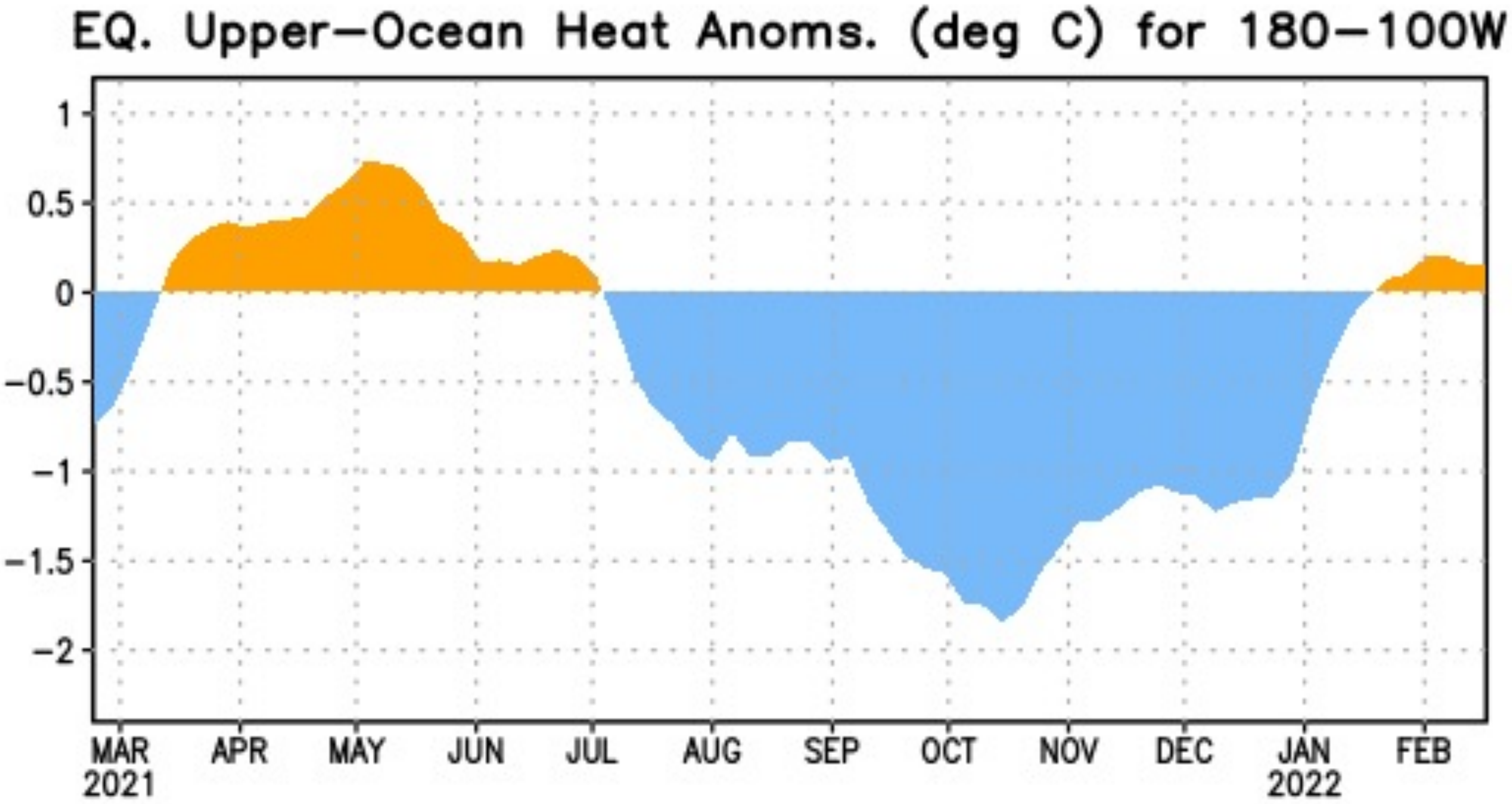

EQ. Upper-Ocean Heat Anoms. (deg C) for 180-100W
1
0.5
0
-0.5
-1
-1.5
-2
MAR
2021
APR
MAY
JUN
JUL
AUG
SEP
OCT
NOV
DEC
JAN
2022
FEB

# Average SST Anomalies
## 22 JAN 2023 – 18 FEB 2023

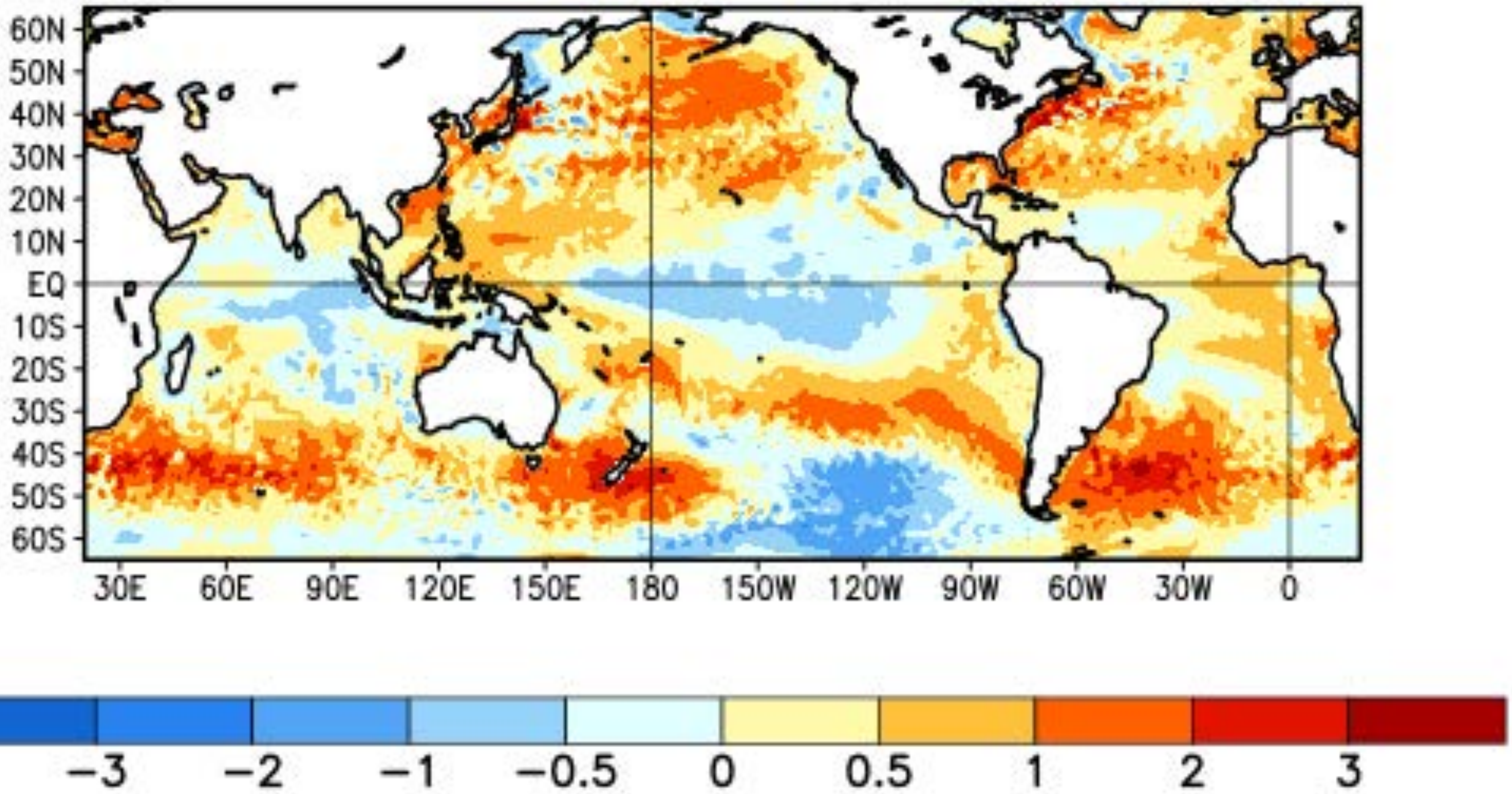

MEI = Weighted spatial patterns of 6 variables (SLP, SST, U, V, T, clouds)
monthly averages + = warm phase (El Nino) – = cold phase (La Nina)

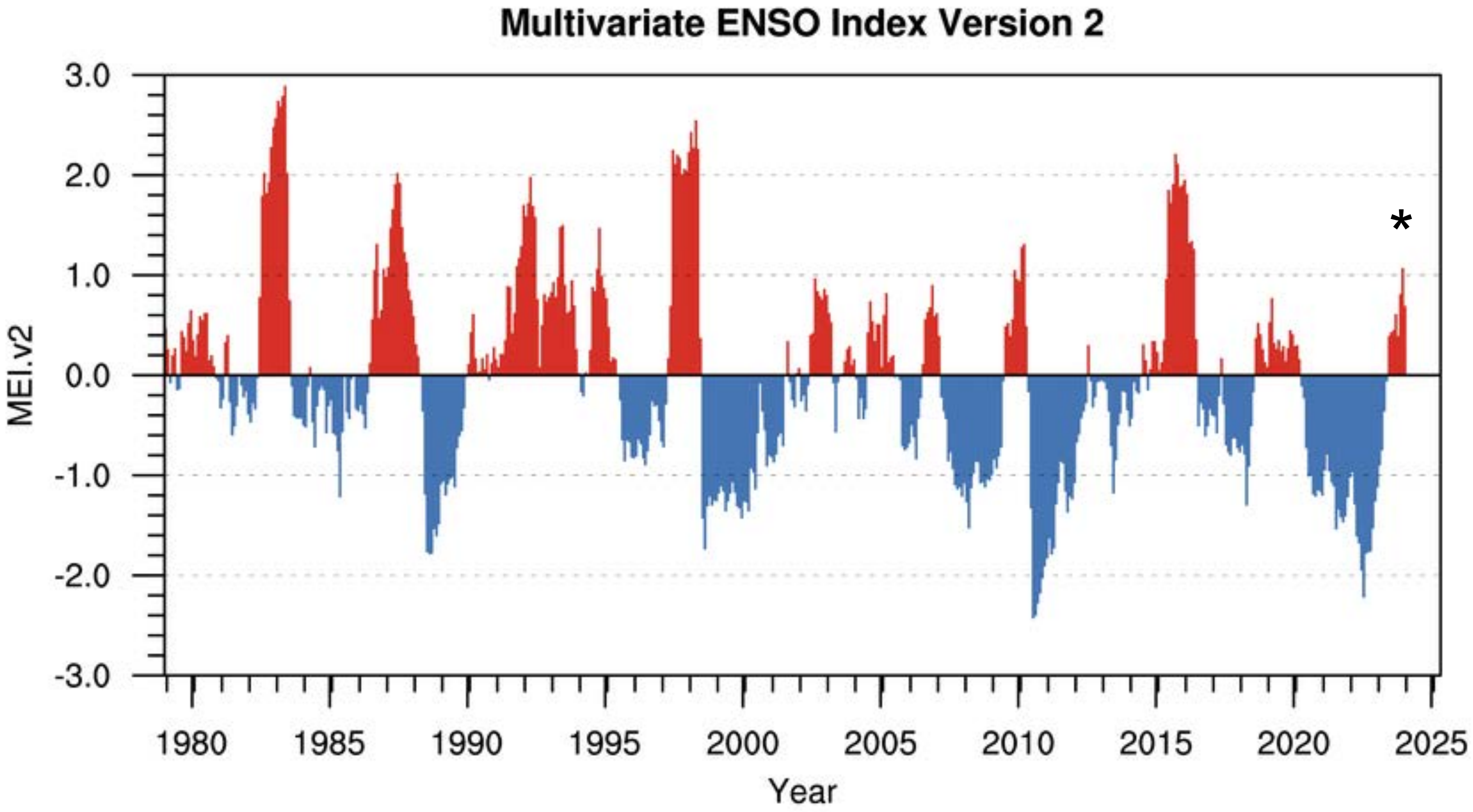

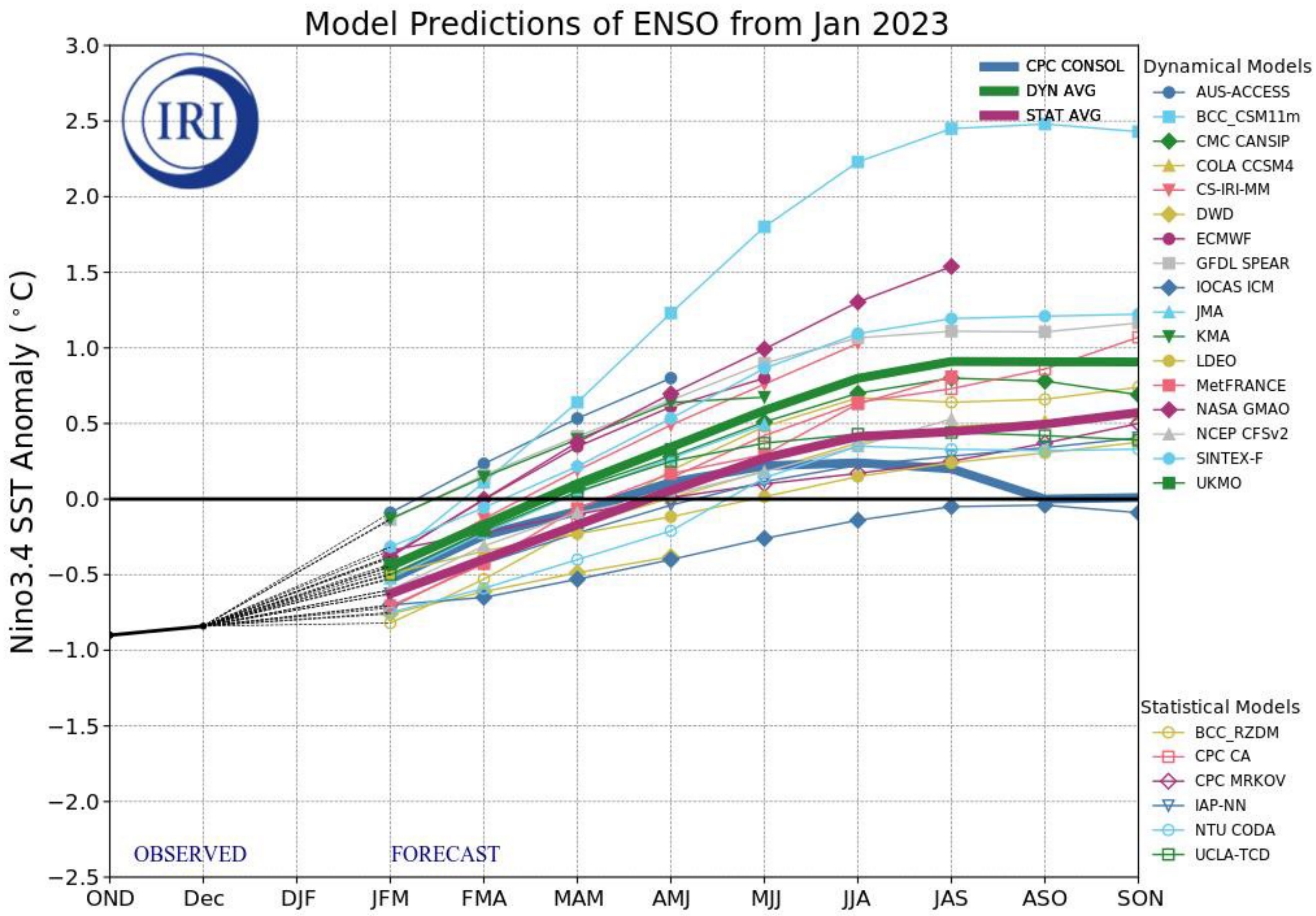

Model Predictions of ENSO from Jan 2023
Nino3.4 SST Anomaly (°C)
IRI
OBSERVED
FORECAST
OND
Dec
DJF
JFM
FMA
MAM
AMJ
MJJ
JJA
JAS
ASO
SON
CPC CONSOL
DYN AVG
STAT AVG
Dynamical Models
AUS-ACCESS
BCC_CSM11m
CMC CANSIP
COLA CCSM4
CS-IRI-MM
DWD
ECMWF
GFDL SPEAR
IOCAS ICM
JMA
KMA
LDEO
MetFRANCE
NASA GMAO
NCEP CFSv2
SINTEX-F
UKMO
Statistical Models
BCC_RZDM
CPC CA
CPC MRKOV
IAP-NN
NTU CODA
UCLA-TCD

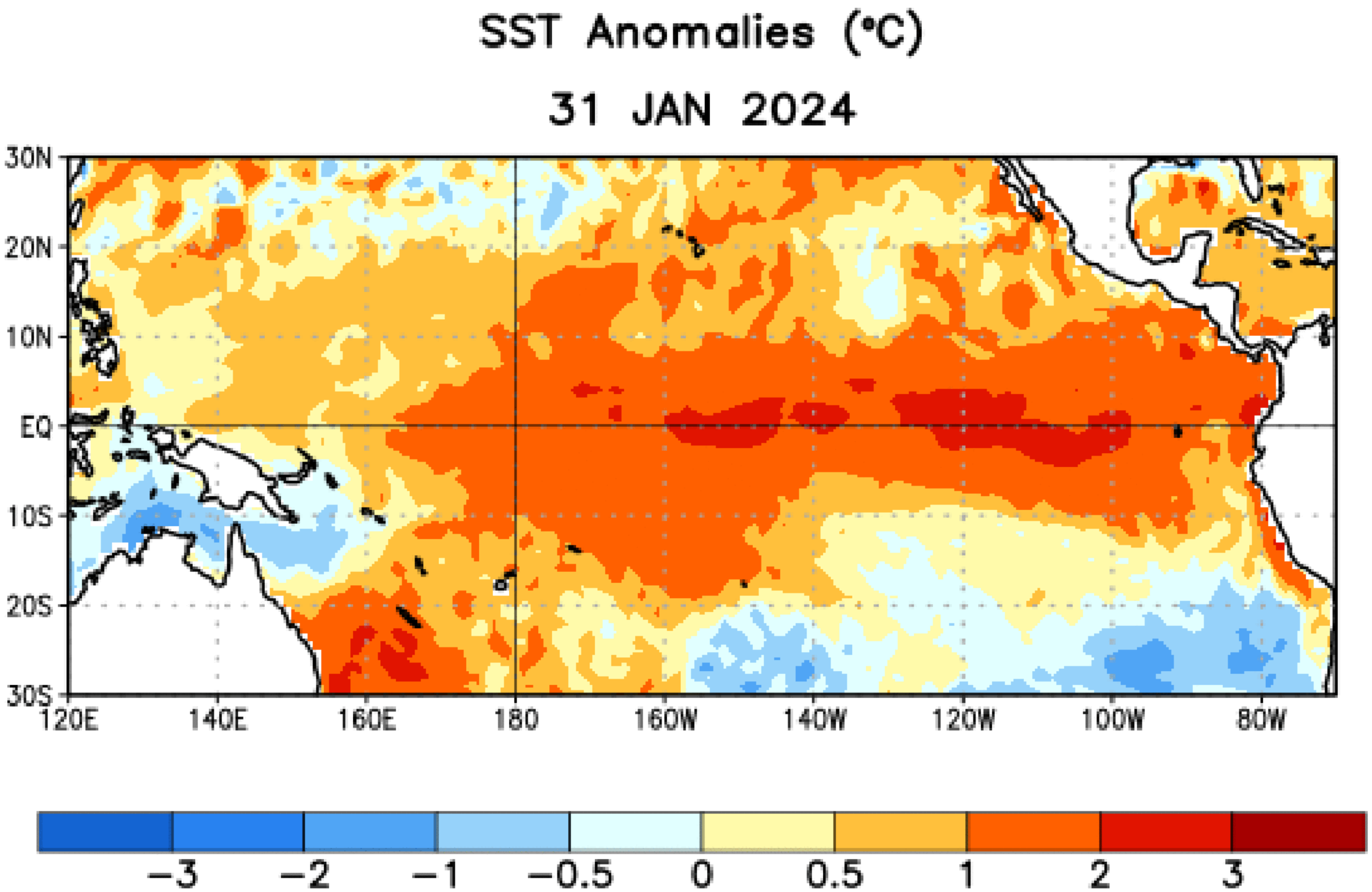


Figure 1. Average sea surface temperature (SST) anomalies (°C) for the week centered on 31 January 2024. Anomalies are computed with respect to the 1991-2020 base period weekly means.

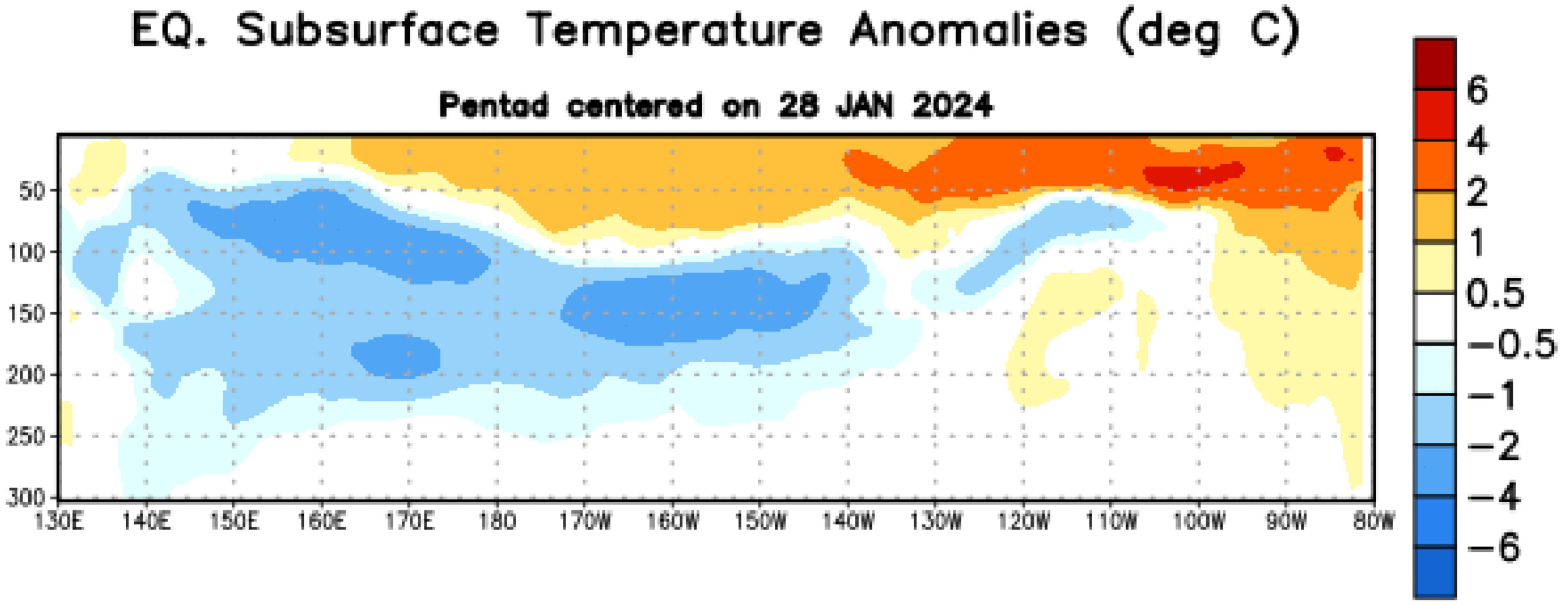


Figure 4. Depth-longitude section of equatorial Pacific upper-ocean (0-300m) temperature anomalies (°C) centered on the pentad of 28 January 2024. Anomalies are departures from the 1991-2020 base period pentad means.

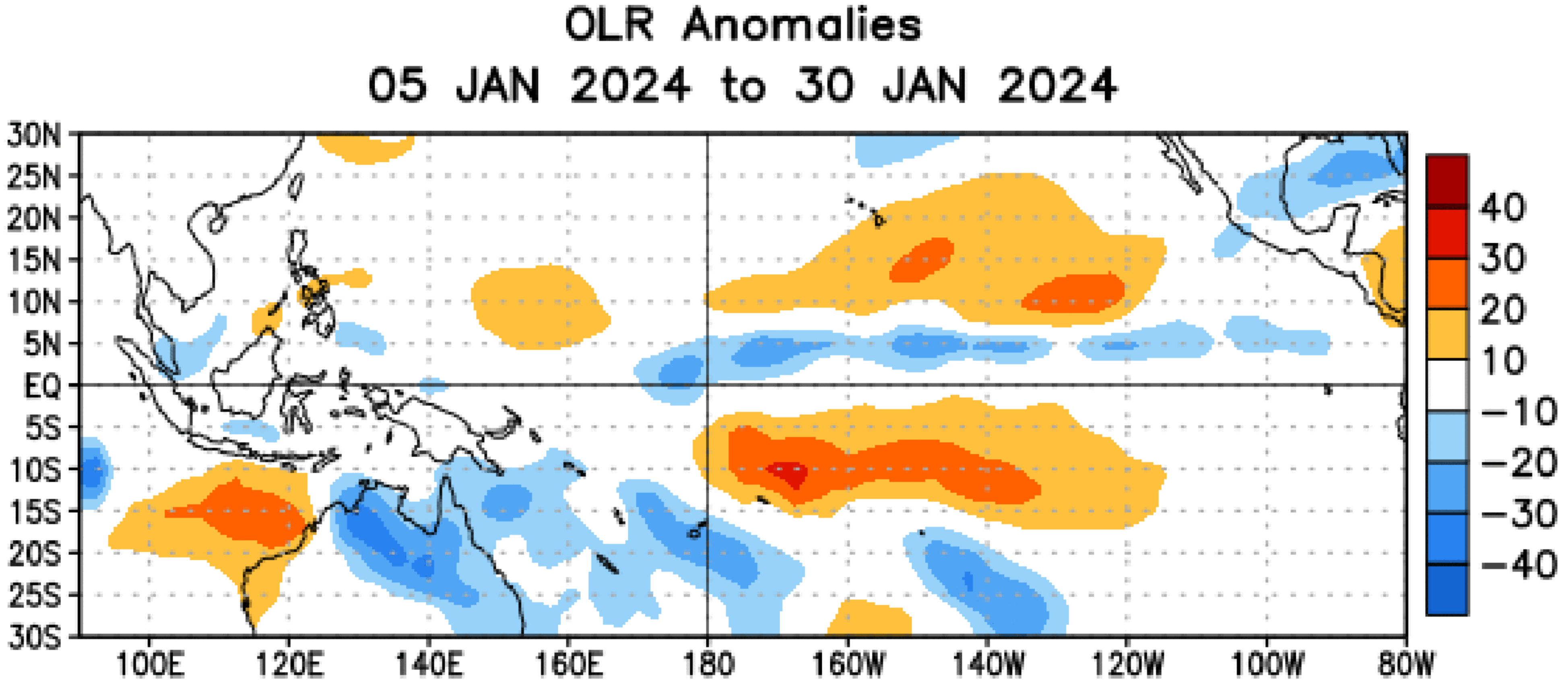


Figure 5. Average outgoing longwave radiation (OLR) anomalies (W/m$^2$) for the period 5 – 30 January 2024. OLR anomalies are computed as departures from the 1991-2020 base period pentad means.

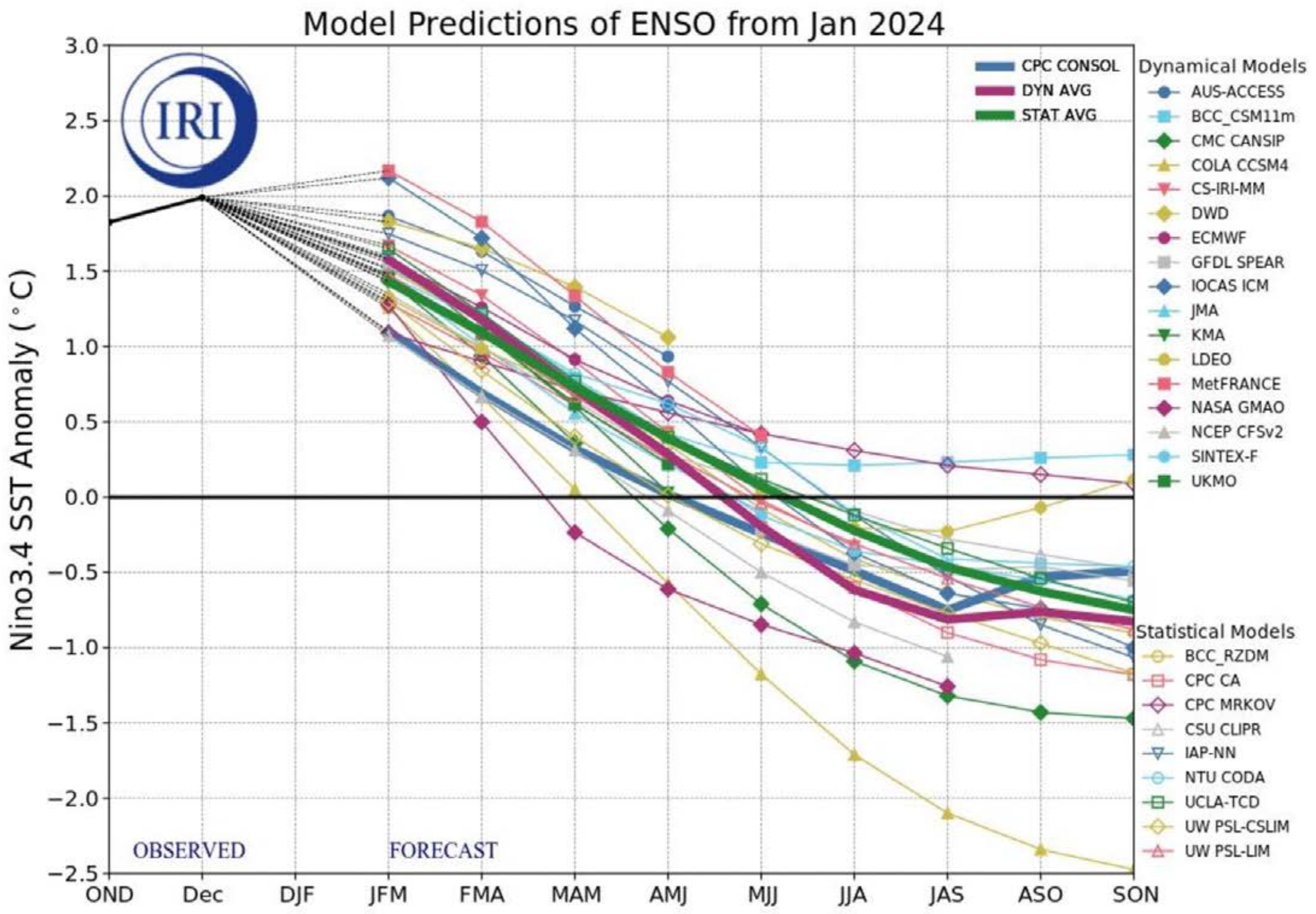


Figure 6. Forecasts of sea surface temperature (SST) anomalies for the Niño 3.4 region (5°N-5°S, 120°W-170°W). Figure updated 19 January 2024 by the International Research Institute (IRI) for Climate and Society.

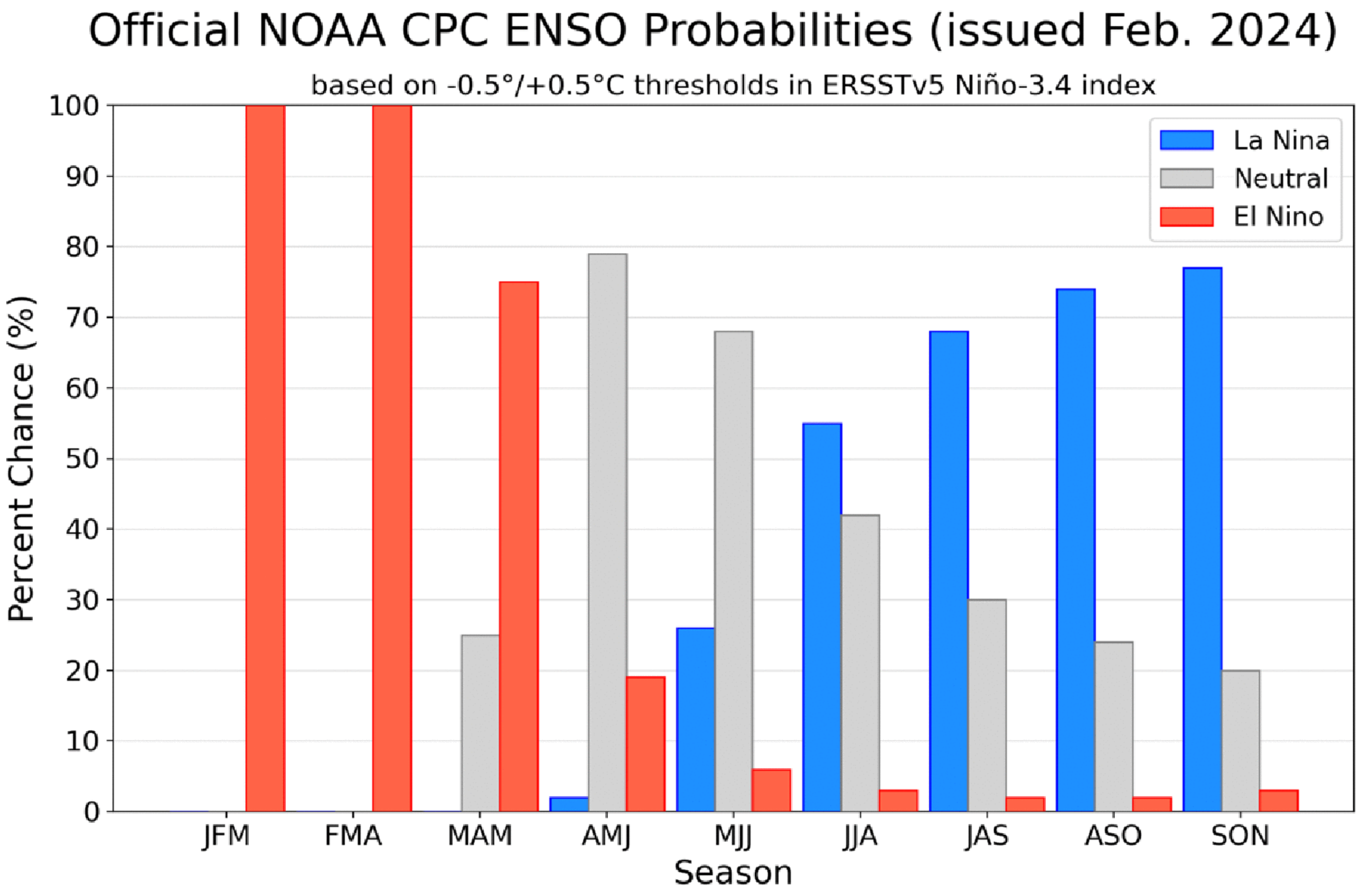


Figure 7. Official ENSO probabilities for the Niño 3.4 sea surface temperature index (5°N-5°S, 120°W-170°W). Figure updated 8 February 2024.

Ensō (円相 , circle)
Zen Buddhism

Symbolizes absolute enlightenment, strength, elegance, the universe, and mu (the void).

**13. ENSO study guide questions**

What is El Nino?

What is the Southern Oscillation?

What are the main characteristics of the tropical atmosphere and the ocean during the cold phase of ENSO (La Nina)?

During the warm phase (El Nino)?

What are some practical reasons for trying to understand and predict ENSO?

nullschool.net - check out today's patterns of winds and SST over the globe